The intraspecific diversity of tooth morphology in the large-spotted catshark Scyliorhinus stellaris : insights into the ontogenetic cues driving sexual dimorphism

Fidji Berio, Allowen Evin, Nicolas Goudemand, Mélanie Debiais-thibaud

ORIGINAL ARTICLE

The intraspecific diversity of tooth morphology in the large-spotted catshark *Scyliorhinus stellaris*: insights into the ontogenetic cues driving sexual dimorphism

Fidji Berio[1,2] | Allowen Evin[1] | Nicolas Goudemand[2] | Mélanie Debiais-Thibaud[1]

[1]Institut des Sciences de l'Évolution de Montpellier, ISEM, Université de Montpellier, CNRS, IRD, EPHE, UMR5554, France

[2]Univ. Lyon, École Normale Supérieure de Lyon, Centre National de la Recherche Scientifique, Université Claude Bernard Lyon 1, Institut de Génomique Fonctionnelle de Lyon, UMR 5242, 46 Allée d'Italie, F-69364 Lyon Cedex 07, France

Correspondence
Mélanie Debiais-Thibaud, Institut des Sciences de l'Évolution de Montpellier, ISEM, Université de Montpellier, CNRS, IRD, EPHE, UMR5554, France
Email: melanie.debiais-thibaud@umontpellier.fr

Funding information
Nicolas Goudemand, ENS de Lyon, "Attractivité Nouveaux Professeurs"

Teeth in sharks are shed and replaced throughout their lifetime. Morphological dental changes through ontogeny have been identified in several species, and have been correlated to shifts in diet and the acquisition of sexual maturity. However, these changes were rarely quantified in detail along multiple ontogenetic stages, which makes it difficult to infer the developmental processes responsible for the observed plasticity. In this work, we use micro-computed tomography and 3D geometric morphometrics to describe and analyze the tooth size and shape diversity across three ontogenetic stages (hatchling, juvenile, and sexually mature) in the large-spotted catshark *Scyliorhinus stellaris* (Linnaeus, 1758). We first describe the intra-individual variation of tooth form for each sex at each ontogenetic stage. We provide a tooth morphospace for palatoquadrate and Meckelian teeth and identify dental features, such as relative size and number of cusps, involved in the range of variation of the observed morphologies. We then use these shape data to draw developmental trajectories between ontogenetic stages and for each tooth position within the jaw to characterize ontogenetic patterns of sexual dimorphism. We highlight the emergence of gynandric heterodonty between the juvenile and mature ontogenetic stages, with mature females having tooth morphologies more similar to juveniles' than mature males that display regression in the number of accessory cusps. From these data, we speculate on the developmental processes that could account for such developmental plasticity in *S. stellaris*.

KEYWORDS
geometric morphometrics, gynandric heterodonty, monognathic heterodonty, ontogenetic trajectory, scyliorhinids

Cite as: Berio, F., Evin, A., Goudemand, N. and Debiais-Thibaud, M. (2020) The intraspecific diversity of tooth morphology in the large-spotted catshark *Scyliorhinus stellaris*: insights into the ontogenetic cues driving sexual dimorphism. *Journal of Anatomy*, 237(5): 960-978. doi: 10.1111/joa.13257.

1 | INTRODUCTION

The fantastic diversity of shark tooth shapes has been studied in relation to the evolutionary history and ecological traits of this iconic group (Bazzi et al., 2018). Functionally convergent tooth shapes between the bonnethead sharks *Sphyrna tiburo* (Sphyrnidae) and horn sharks (Heterodontidae) were associated with the hard prey they feed on (Wilga and Motta, 2000). On the other hand, a strong phylogenetic signal arose from the analysis of the whole dentition of Lamniforms, which have a unique symphyseal to commissural tooth-type patterning (Shimada, 2002, 2005). For this reason, tooth shape is one of the main supports for establishing taxonomic groups and phylogenetic relationships between fossil and extant elasmobranchs (sharks and batomorphs) (Shimada, 2002, 2005; Cappetta, 2012). One issue in this matter arises from the fact that an elasmobranch is rarely characterized by a single tooth type (molariform, unicuspidate, multicuspidate) within the jaw but by a continuum of different tooth shapes along the jaw axis (monognathic heterodonty) and often displays differences between the palatoquadrate (upper) and Meckelian (lower) teeth (dignathic heterodonty). The continuous and lifelong replacement of teeth in elasmobranchs makes this variation dynamic in time (ontogenetic heterodonty), their tooth types being replaced, linked to dietary shifts (Luer et al., 1990; Powter et al., 2010) and reproductive status (Reif, 1976; Springer, 1979; Gottfried and Francis, 1996; Motta and Wilga, 2001; Purdy and Francis, 2007; Powter et al., 2010; French et al., 2017).

In elasmobranchs, tooth replacement occurs at various rates and following different patterns, depending for instance on tooth imbrication and water temperature, and may also differ between jaws (Strasburg, 1963; Luer et al., 1990; Correia, 1999; Moyer and Bemis, 2016; Meredith Smith et al., 2018). Gynandric heterodonty (sexual dimorphism in teeth) is very common in elasmobranchs (Feduccia and Slaughter, 1974; Taniuchi and Shimizu, 1993; Kajiura and Tricas, 1996; Geniz et al., 2007; Gutteridge and Bennett, 2014; Underwood et al., 2015; French et al., 2017) and affects specific tooth files (reported in Dasyatidae, Carcharhinidae, and Leptochariidae) to the whole dental set at various degrees during the sexually mature stage (Cappetta, 1986). The higher and sharper mature male teeth are indeed assumed to function in grasping females and consequently to facilitate clasper introduction during copulation (Springer, 1966; McEachran, 1977; McCourt and Kerstitch, 1980; Cappetta, 1986; Ellis and Shackley, 1995; Kajiura and Tricas, 1996; Pratt, Jr. and Carrier, 2001; Litvinov and Laptikhovsky, 2005; Gutteridge and Bennett, 2014). This feature has been recorded as a seasonal variation in the Atlantic stingray *Dasyatis sabina* (Kajiura and Tricas, 1996), while it is assumed to be a fixed-in-time feature in other elasmobranch species for which it has been described (Gutteridge and Bennett, 2014; de Sousa Rangel et al., 2016). Gynandric heterodonty has also been only described at sexually mature stages, suggesting that sex hormone signals triggering the reproductive activity may also be involved in the development of the observed dental sexual dimorphism (McEachran, 1977; Cappetta, 1986; Snelson et al., 1997; Powter et al., 2010).

Shark tooth shapes have been mostly evaluated through semi-quantitative studies based on asymmetry, number, sharpness, and relative bending or size of cusps (Cappetta, 1986; Frazzetta, 1988). Moreover, studies that performed morphometrics on extant species mainly focused on tooth crown dimensions (height, width, and angle) of specific teeth (small-spotted catshark *Scyliorhinus canicula* (Linnaeus, 1758) (Ellis and Shackley, 1995), Lamniforms (Shimada, 2002), and Port Jackson shark *Heterodontus portusjacksoni* (Meyer, 1793) (Powter et al., 2010)). These approaches mainly base the tooth shape analysis on main cusp dimensions, which do not capture complex heterodonty patterns (Whitenack and Gottfried, 2010). Recent publications, however, have fo-

cused on quantitative tooth traits in sharks by using geometric morphometrics (Marramà and Kriwet, 2017; Soda et al., 2017; Cullen and Marshall, 2019), providing more subtle information on tooth size and shape quantitative variation. These comparative studies allow to infer developmental and phylogenetic hypotheses and refine our knowledge about the inter- and intraspecific tooth shape variation in several shark species. Overall, the authors highlight the benefits of a quantitative investigation of complete tooth shape patterns in sharks to understand ontogenetic and evolutionary shifts.

Scyliorhinids are emerging models for shark studies (Coolen et al., 2008) and among them, *S. canicula* tooth morphologies have been the most studied. Mature *S. canicula* specimens display gynandric heterodonty that has been qualitatively described (Brough, 1937; Ellis and Shackley, 1995; Erdogan et al., 2004; Debiais-Thibaud et al., 2015; Soares and Carvalho, 2019) but quantification of scyliorhinids dental variation is still fragmentary. In particular, the nursehound *Scyliorhinus stellaris* (Linnaeus, 1758) is a phylogenetically close relative of *S. canicula* (Iglésias et al., 2005; Vélez-Zuazo and Agnarsson, 2011) and has mostly been studied for physiological aspects (Piiper et al., 1977; Heisler and Neumann, 1980). To our knowledge, the study of Soldo et al. (2000) is the only one focusing on *S. stellaris* tooth shape patterns. However, this study did not test the impact of ontogeny on tooth morphology and did not detect sexual dimorphism although gynandric heterodonty is known to be a common feature to Scyliorhinidae (Cappetta, 1986; Soldo et al., 2000; Soares and Carvalho, 2019).

Here, we provide the first detailed description of *S. stellaris* tooth form (shape and size) using microCT images and quantitative 3D geometric morphometrics. We characterize the ontogenetic and sexually dimorphic trajectories of tooth shapes and highlight the emergence of gynandric heterodonty with sexual maturation. We also describe intra-individual tooth morphological variation and we discuss the developmental hypotheses that could be involved in the observed tooth diversity of *S. stellaris*.

2 | MATERIALS AND METHODS

2.1 | Biological material

In total, 33 specimens of *S. stellaris* (16 females, 17 males; 2,467 teeth) were analyzed. Total length (TL, in cm) was used to define the groups of same ontogenetic stages. Female *S. stellaris* are considered sexually mature at 79 cm TL and males at 77 cm TL (Fischer et al., 1987; Musa et al., 2018) but longer mature specimens were chosen to avoid biases due to potential later maturation. Juveniles were twice shorter than the mature specimens and hatchling specimens were chosen as close as possible from hatching (Musa et al., 2018) although umbilical scars were never observed. We cannot evaluate how these time points are distributed along the ontogeny of the specimens because we have no information on the age of each specimen, and no growth curve has been published for this species beyond the hatchling stage (Musa et al., 2018). Growth rates may be sex-specific in elasmobranchs (Hale and Lowe, 2008) so we may expect age differences between males and females of similar total length. Hatchling specimens were 17.7cm ± 3.3cm TL (7 females, 5 males), juveniles were 57.7cm ± 3.2cm TL (5 females, 5 males) and mature ones were 102.7cm ± 7.2cm TL (4 females, 7 males) (Table 1). Dried jaws were provided by the Institute of Evolution Sciences of Montpellier (France) and jaws preserved in ethanol were provided by the Aquarium du Cap d'Agde (France).

2.2 | MicroCT scans

Jaws were microCT scanned using a Phoenix Nanotom S with voxel sizes ranging from (10.7μm) to (30.0μm) and 3D volumes were reconstructed using the corresponding phoenix datos x2 reconstruction software (v2.3.0).

2.3 | Tooth selection

For each specimen, all 3D teeth were isolated from the right palatoquadrate and Meckelian cartilages with Amira software (v6.2.0) (Stalling et al., 2005). Each tooth was identified within a file (or family) along the mesio-

distal axis and by the generation within a tooth file (Fig. 1A). Within each tooth file, we analyzed 1 to 4, functional but not worn, generations.

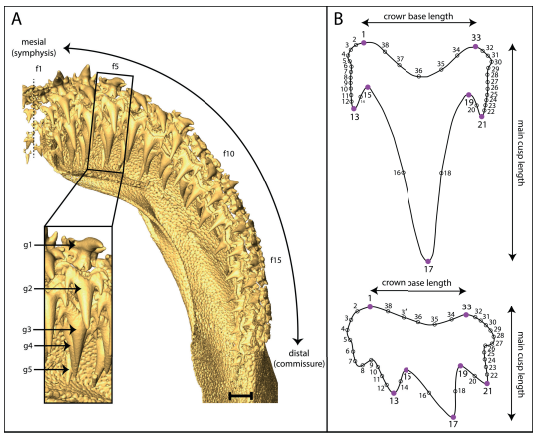

FIGURE 1 Tooth identification within a jaw and landmarking. A) microCT image of a right Meckel's cartilage of a juvenile female *S. stellaris*, dorsal view. f, file as defined from the symphysis (dotted line) to the commissure; g, generation. Scale bar represents 2.5mm for the jaw and 1mm for the zoomed teeth; B) Mesial (top) and distal (bottom) examples of landmark (purple) and semilandmark (empty dots) setting.

The teeth were not clustered into classically used tooth-type denominations (e.g., symphyseal, parasymphyseal, lateral, commissural) (Reif, 1976; Lucifora et al., 2001) on purpose since we did not visually identify abrupt tooth shape or size change along the mesio-distal axis, except for the symphyseal teeth on the lower jaw (Fig. 1A). These symphyseal teeth are located between the right and left Meckelian cartilages and are not located above jaw cartilages, contrary to all other teeth. All subsequent analyses were performed under the hypothesis of homology between tooth files of different specimens, which for example means that the most symphyseal Meckelian tooth file of a given hatchling male is considered equivalent to the most symphyseal Meckelian tooth file of a mature female.

2.4 | Geometric morphometrics

Seven 3D landmarks and 31 semilandmarks were placed on the cutting edge of each tooth (Fig. 1B) with the Landmark software (v3.0.0.6) (Wiley et al., 2005) and the data were preprocessed with Scyland3D (v1.1.0) (Berio and Bayle, 2020). The semilandmark density was made higher in the lateral sides of the teeth because gynandric heterodonty in scyliorhinids is known to involve the addition of lateral accessory cusps (Gosztonyi, 1973; Ellis and Shackley, 1995; Debiais-Thibaud et al., 2015; Soares and Carvalho, 2019). Our form comparison analyses will be interpreted in light of this choice: the centroid size and shape parameters will be more affected by variations in the lateral zones (with higher density of semilandmarks) than in the main cusp and crown base zones. All analyses were performed separately for Meckelian and palatoquadrate teeth.

Crown base width was computed based on the distance between landmarks 1 and 33 (d1-33, Fig. 1B), while main cusp height was the mean of the distances between the main cusp and each side of the tooth (mean of d1-17 and d17-33, see Fig. 1B). We also used these measures to generate a ratio between main cusp height and crown base width, later referred to as the cusp-crown ratio. Tooth symmetry was measured by the ratio between d1-17 and d17-33 and a value of 1 implies a symmetric tooth.

A Generalized Procrustes Superimposition (GPA) was performed (Bookstein, 1991) during which the semilandmarks were slided based on minimizing bending energy (Bookstein, 1997). The tooth size patterns were investigated using centroid sizes computed based on the GPA and the tooth shape variation was displayed with principal component analyses (PCAs). In order to reduce the high dimensionality of the aligned coordinates, the data were reduced prior to multivariate analyses of variance (MANOVAs) to the axes containing 95% of the total variation (14 and 13 PCA axes for Meckelian and palatoquadrate teeth respectively, out of 114 available axes). We defined the random variable as the tooth generation within a given tooth file, in a specimen. We used these generations as internal replicates from which we gen-

erated an average tooth shape per tooth file, for each specimen. One-Way analyses of variance (ANOVAs) and MANOVAs were then computed on tooth mean centroid size and tooth shape for each tooth position, each sex, at each ontogenetic stage, to avoid biases due to unbalanced sampling between tooth files (from one to four sampled teeth within one tooth file). Two-way ANOVAs and MANOVAs were subsequently used on tooth mean centroid size and shape to test the interaction between sex, stage, and tooth position along the jaw. Within each jaw, inter-group differences in shape were first investigated between sexes without considering ontogenetic stages nor tooth positions. The differences due to sex and tooth position within the jaw were subsequently tested within given ontogenetic stages.

Trajectory analyses were performed to evaluate the developmental tooth shape changes within each tooth position. The trajectories were computed and compared i) between sexes and ii) between two consecutive ontogenetic stages within sexes (e.g., from hatchling to juvenile, and juvenile to mature). The statistical tests were performed on the length, direction, and shape of the trajectory in the morphospace (Adams and Otárola-Castillo, 2013).

Geometric morphometric superimposition and analyses were carried out in R (v3.4.3) with the geomorph library (v3.2.1) (Adams and Otárola-Castillo, 2013).

3 | RESULTS

3.1 | Visual inspection of tooth morphology

There were no symphyseal teeth on the palatoquadrate, but one symphyseal file on the Meckelian cartilage (for 41% of the specimens). Although the second Meckelian tooth file is partially located above the Meckelian mesial edge, the teeth display size and morphological similarities to the symphyseal ones (for 59% of the specimens). We report no significant difference in tooth file counts between right and left sides of the jaw within each ontogenetic stage for each sex (Wilcoxon matched-pairs signed rank tests, p-val$> 4.60e^{-2}$ for all tests; we observed a maximum difference of two tooth files between the right and left jaws, in 13/51 comparisons). Palatoquadrate number of tooth files does not differ significantly between ontogenetic stages in males and in females (One-Way permutation ANOVAs, p-vals $> 5.00e^{-2}$). Conversely, in both sexes, there are significantly more Meckelian tooth files in juvenile and mature specimens compared to hatchling ones (One-way permutation ANOVAs, p-vals $< 5.00e^{-2}$), but no difference was detected between the juvenile and mature ontogenetic stages. Moreover, there is no significant difference in tooth file counts between males and females (Wilcoxon tests, p-val$> 3.10e^{-1}$ for all tests).

A graded decrease of tooth size is observed along the mesio-distal axis of the jaw, except for the symphyseal teeth which are smaller than parasymphyseal ones (see Fig. 1, Fig. 2E, and Fig. 3E and I). In all sexes and stages, there is a graded increase of lateral bending of teeth from the symphysis to the commissure, producing asymmetric teeth (Fig. 2 and 3). Teeth of male and female hatchlings are visually similar in shape with tricuspid teeth in both jaws (Fig. 2A to D and Fig. 3A to D).

Juvenile female and male teeth display little variability in cusp number along the jaw: mesial palatoquadrate teeth (Fig. 2E) often display one main cusp and four accessory cusps while the more distal ones have four to five cusps and often more accessory cusps in the mesial than in the distal part of the crown (Fig. 2E to H). A similar pattern is observed in Meckelian teeth (Fig. 3E to H), except for tricuspid symphyseal ones. Mature female teeth are similar in shape to those of juveniles except at the most distal positions where they exhibit up to six cusps (Fig. 2I to L and Fig. 3I to L). Mature male mesial teeth are always un-bent and unicuspidate while more distal teeth undergo an addition of one to two accessory cusps (Fig. 2M to P and Fig. 3M to P). Mature male teeth rarely display more than two accessory cusps (Fig. 2M to O and Fig. 3M to P), however a small third accessory cusp was detected on the distalmost teeth of some specimens (see arrow on Fig. 3P).

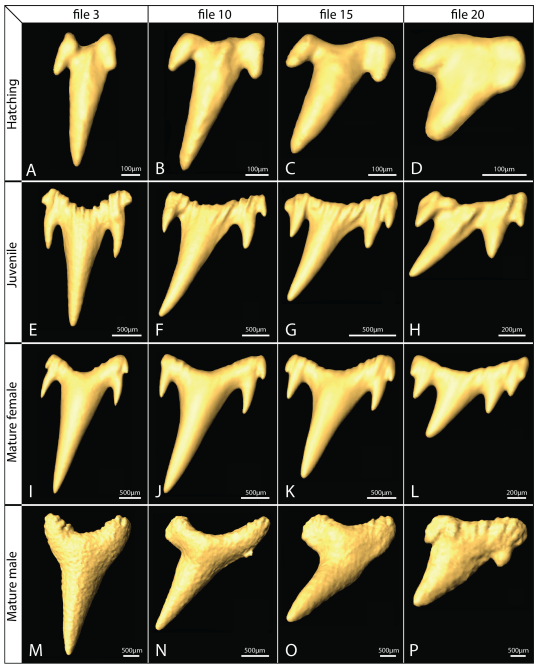

FIGURE 2 Palatoquadrate tooth shape diversity in *S. stellaris*. A-D) Hatchling female teeth; E-H) Juvenile female teeth; I-L) Mature female teeth; M-P) Mature male teeth. Symphyseal (mesial) pole to the left.

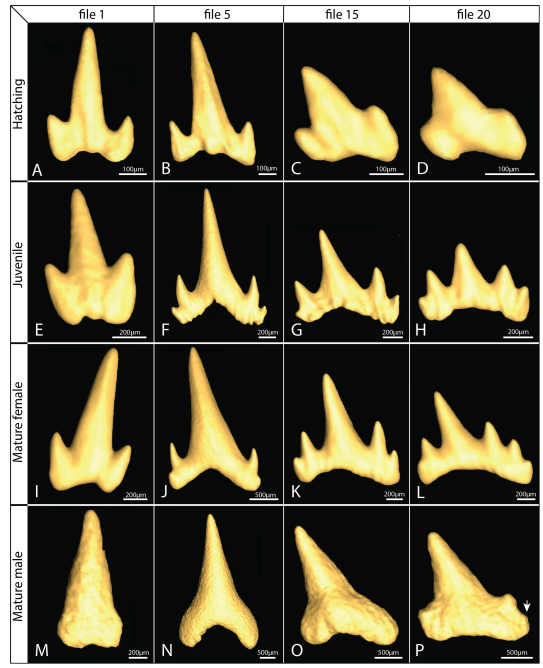

FIGURE 3 Meckelian tooth shape diversity in *S. stellaris*. A-D) Hatchling female teeth; E-H) Juvenile female teeth; I-L) Mature female teeth; M-P) Mature male teeth. Symphyseal (mesial) pole to the left.

3.2 | Morphometric analyses

3.2.1 | Tooth size patterns

To support and quantify visual observations, morphometric measurements were performed and ratios of the main cusp height and the crown base width were computed. Ratio values are higher than 1, showing that the main cusp is higher than the crown base is wide (Fig. 4A and D).

In all groups, this ratio decreases along the mesio-distal axis of the jaw (Fig. 4A and D), with exceptions in the distalmost positions in Meckelian teeth of mature males and juvenile females (Fig. 4A and D). The variation of this ratio follows the gradual decrease of both measures, although stronger decrease is observed in the main cusp height (Additional figure). At each position, the measured cusp-crown ratio is very comparable between ontogenetic stages, but in the palatoquadrate teeth of hatchling specimens we report higher ratios (1.5-fold increase), with a minimum of 1.6 along the mesio-distal axis (see position 19 in hatchling males in Fig. 4D). The raw data on main cusp height and crown base width show that hatchling palatoquadrate teeth are different from Meckelian teeth because of their smaller crown base (Additional figure, A and B). Overall, these observations point to similar developmental constraints on the overall geometry of teeth at all ontogenetic stages on Meckelian teeth and to a transition of these developmental constraints between the hatchling and juvenile ontogenetic stages in palatoquadrate teeth.

3.2.2 | Tooth asymmetry

Teeth of *S. stellaris* undergo a global increase of bilateral asymmetry from the symphysis to the commissure al-

though we also report a sudden fall of asymmetry values in the distalmost tooth files (Fig. 4B and E). In Meckelian teeth, the tooth asymmetry values of all groups (ontogenetic stages) are overlapping until the 15th tooth file, but female teeth distal to this position tend to display higher asymmetries than teeth of other groups (Fig. 4B). A similar pattern is observed in the palatoquadrate: asymmetry values of all groups are very similar until the 14th tooth file (Fig. 4E). However, contrary to Meckelian teeth, asymmetry patterns of hatchling teeth distal to the 14th tooth file are distinct from those of juveniles with lower asymmetry values (Fig. 4E). Mature males display teeth whose symmetry values are in between those of hatchling and juvenile specimens (Fig. 4E). As for Meckelian teeth, mature female teeth are the most asymmetrical (Fig. 4E) with maximum values between the 19th and 23rd files (Fig. 4B). In the palatoquadrate, these maxima are reached between the 22nd and 24th tooth files in all groups (Fig. 4E). We also highlight that the anteriormost teeth (1st file in the palatoquadrate and up to the 3rd file in the Meckelian cartilage) are close to bilateral symmetry (Fig. 4B and E). These measurements highlight similar tooth mesio-distal asymmetry patterns within hatchling and juvenile specimens and higher asymmetry values in mature females compared to all other groups (Fig. 4B and E).

3.3 | Geometric morphometric analyses

In the previous two morphometric analyses, the mesio-distal variation of tooth shape could be discriminated in terms of relation of cusp height and crown width and in terms of asymmetry for juvenile and mature teeth. However, no strong difference of these parameters could be seen between sexes in either jaws of all three ontogenetic stages. In the following, we established the tooth centroid size patterns of variation along the mesio-distal jaw axis for each group.

Meckelian teeth. Both sexes show similar tooth centroid size patterns along the mesio-distal axis of the jaw at hatchling and juvenile stages (Fig. 4C). Hatchling males and females display very little tooth centroid size variation along the jaw (Fig. 4C), as opposed to juvenile and mature specimens that share a maximum tooth centroid size in file 5 or 6 (Fig. 4C): values for juvenile teeth are intermediate between the hatchling and mature values. Overall, the mesio-distal tooth centroid size pattern is similar between juvenile and mature specimens (Fig. 4C) but mature males display an exacerbated tooth size pattern compared to mature females, except at the symphyseal tooth positions (Fig. 4C).

Palatoquadrate teeth. Similar to the Meckelian teeth, palatoquadrate tooth centroid sizes do not differ between sexes at hatchling or juvenile stages, centroid size increase with ontogenty, and mature males display higher values compared to females (Fig. 4F). Juvenile males and females have two local maximum tooth centroid sizes at the 3rd and 12th and 4th and 10th files respectively, and a minimum centroid size at file 7 (Fig. 4F). Mature specimens display a clear bimodal tooth centroid size pattern from the symphysis to the commissure, with local maximum values in the 3rd and 10th files and a local minimum value in the 7th file (Fig. 4F). Topologically, the Meckelian file 5 (maximal value in adult males) faces the palatoquadrate file 7 (local minimum in adult males) which suggests functional constraints for these variation of tooth size along the mesio-distal axis.

Our statistical tests corroborated the observation that tooth centroid size varies according to the ontogenetic stage in both cartilages (One-Way ANOVAs, p-vals $< 2.00e^{-16}$, Table 2). Within all ontogenetic stages, the Meckelian and palatoquadrate tooth mesio-distal position also significantly impacts the tooth centroid size (One-Way ANOVAs, p-vals $< 9.37e^{-4}$, Table 2). The Meckelian and palatoquadrate tooth centroid size of mature specimens is also significantly impacted by sex (One-Way ANOVAs, p-vals $< 1.54e^{-2}$, Table 2). We finally report a significant interaction between sex and ontogenetic stage in the Meckelian and palatoquadrate full datasets (Two-Way ANOVAs, p-vals $< 3.24e^{-3}$, Table 2), as well as between ontogenetic stage and tooth mesio-distal position in Meckelian teeth (Two-Way ANOVA, p-val$< 2.49e^{-3}$, Table 2).

3.4 | Developmental trajectories

We performed independent PCAs in each jaw, and the extreme shapes on the PC1 and PC2 axes illustrate how similar shape parameters generate the main Meckelian and palatoquadrate variations of tooth shapes. This first observation highlights the fact that, although we treated them separately, teeth of the upper and lower jaw show similar shape variations along the first PCs. In both cases, the main axis of tooth shape variation relates to the main cusp proportions, and to the variation in the number of lateral accessory cusps (Fig. 5A and 5B). The second axis of variation seems to relate to the size of lateral cusps relative to the main cusp size (Fig. 5A and 5B).

The shape of Meckelian and palatoquadrate teeth of *S. stellaris* is mostly impacted by ontogenetic stage (One-Way MANOVAs, pvals$< 2.20e^{-16}$, $3.04e^{1}$ <F approx< $4.58e^{1}$, Table 3) although the sex of the specimens and the tooth position along the mesio-distal axis of the jaw also significantly impact the tooth shape (One-Way MANOVAs, Sex: p-val$< 6.13e^{-8}$, 5.39<F approx<7.61; Tooth position: p-val$< 3.12e^{-14}$, 1.80<F approx<1.89, Table 3). Within ontogenetic stages, the mesio-distal position of a tooth significantly impacts the tooth shape of juveniles (One-Way MANOVAs, p-vals $< 1.16e^{-4}$ for both jaws, Table 3) and palatoquadrate teeth of hatchling specimens (One-Way MANOVA, p-val$< 2.28e^{-6}$, Table 3). Conversely, for both jaws and within each ontogenetic stage, a sexual dimorphism of tooth shape was detected (One-Way MANOVAs, p-vals $< 5.37e^{-3}$, Table 3). We finally report that the sexual dimorphism differs between stages and tooth mesio-distal positions for Meckelian and palatoquadrate teeth (Two-Way MANOVAs, p-vals $< 1.02e^{-2}$, Table 3).

Comparison of developmental trajectories between sexes. The full shape developmental trajectories (from hatchling to juvenile, and to mature stage) differ between sexes for most of the palatoquadrate tooth files that are distal to the 3rd file and for all Meckelian tooth files distal to the 8th file (p-vals $< 1.60e^{-2}$, Tables 4 and 5). These differences arise from divergent juvenile-to-mature developmental directions between males and females (45/46 significant p-values, p-vals $< 3.10e^{-2}$, Tables 4 and 5). Significant differences between males and females for juvenile-to-mature trajectory lengths are also reported for most tooth files and always involve longer trajectories in males than females (p-vals $< 3.40e^{-2}$, Tables 4 and 5). We report no such differences between male and female hatchling-to-juvenile trajectory lengths and angles (Tables 4 and 5). This pattern highlights a shift between male and female tooth shape developmental trajectories only after the juvenile stage.

Comparison of developmental trajectories within sexes. Significant differences were observed for all tooth files of both jaws between the hatchling-to-juvenile and the juvenile-to-mature trajectory angles within sexes (p-vals $< 1.20e^{-2}$, Additional tables 1 and 2), showing that whatever the mesio-distal position of a tooth, the shape modifications between juvenile and mature stages cannot be considered a prolongation of the hatchling-to-juvenile modifications. Significant differences in trajectory lengths are reported for most female palatoquadrate files (19/25 significant p-values, Additional table 1) and for female Meckelian files distal to the 8th file (pvals$< 4.40e^{-2}$, Additional table 2). In all these cases, the hatchling-to-juvenile trajectory is longer than the juvenile-to-mature one (Additional tables 1 and 2), showing that, in females, tooth shapes generated at sexual maturation are less dissimilar to juveniles than in males. In contrast, male trajectory lengths significantly differ only in a few tooth files (6/46 significant p-values, Additional tables 1 and 2, p-vals $< 4.60e^{-2}$).

4 | DISCUSSION

4.1 | Capturing the intra-individual and ontogenetic-stage variations of tooth shape in *Scyliorhinus stellaris*

In this study, we generated 3D images and collected 3D coordinates of landmarks and semilandmarks on the cutting edge of the tooth surface. Despite the 3D nature of the surface data, the described tooth outline finally includes very little information in the third dimension.

While the use of 2D data would have probably been less time-consuming, working on 3D data avoids biases due to parallax (Mullin and Taylor, 2002; Fruciano, 2016). Moreover, 3D surfaces can provide insights into topological aspects such as ornamentations, which can be of interest for future studies.

From our analyses, we described the wide range of blade-shaped to crown-shaped teeth in *S. stellaris*, which we characterized through classical and geometric morphometric analyses. In *S. stellaris*, we quantified how classical tooth shape parameters (asymmetry and cusp-crown ratio) vary in a gradual and linear way along the mesio-distal axis of both jaws, with extreme variations at the mesial-most and distal-most tooth positions. Also, we captured a higher cusp-crown ratio for palatoquadrate hatchling teeth compared to other ontogenetic stages. Because the lack of asymmetry is a shared feature of hatchling teeth and symphyseal teeth of older specimens, we show that palatoquadrate and Meckelian teeth undergo similar transition in their development (asymmetry) once the hatching stage is passed, to the exception of the symphyseal teeth. According to visual observations, the palatoquadrate and Meckelian teeth of *S. stellaris* are very similar in shape (dignathic homodonty or weak dignathic heterodonty), which is consistent with previous works on scyliorhinids (Herman et al., 1990; Ellis and Shackley, 1995; Soares and Carvalho, 2019). As opposed to Scyliorhinidae, dignathic heterodonty is very common in other shark groups, such as in Hexanchidae and most Squaliformes. The tooth-type discrepancies between palatoquadrate and Meckelian teeth have been correlated with different functions in feeding: upper grasping teeth might help catching and holding a prey, whereas blade-shaped lower teeth might function in tearing a prey to pieces (Cappetta, 1986; Frazzetta, 1988; Cappetta, 2012). Beyond ecology, dignathic heterodonty might also convey a phylogenetic signal: sharks from distinct taxonomic groups might have overlapping trophic habits (especially in the case of opportunistic behavior) and, however, display different dignathic heterodonty patterns that diet alone cannot explain. Regarding whether the gynandric heterodonty follows similar patterns between both jaws, the data gathered hitherto on sharks are insufficient to answer.

Our results notably suggest a developmental transition between hatchlings and juveniles, especially on the palatoquadrate, that involves a global increase of the crown size. Note that asymmetry and cusp-crown ratio poorly discriminate between the three ontogenetic stages because they are corrected for size. As expected, the variation of tooth centroid size strongly discriminates between ontogenetic stages (Table 2) and shape analyses also recover growth stage significant differences (Table 3).

4.2 | The ontogenetic tempo and pattern of gynandric heterodonty

In previous works, classical shape parameters did not discriminate sex-dependent variation of tooth shape in *S. stellaris*, although gynandric heterodonty is well-known in scyliorhinids (Gosztonyi, 1973; Ellis and Shackley, 1995; Cappetta, 2012; Debiais-Thibaud et al., 2015; Soares and Carvalho, 2019). In our geometric morphometric analyses of *S. stellaris* teeth, we detected no significant centroid size differences between sexes at hatching and juvenile ontogenetic stages, while we observed such difference at mature stages with male tooth centroid sizes being larger than female ones. Centroid size is, per construction, a feature with little sensitivity to shape. However, because we weighted tooth zones by positioning the majority of semilandmarks in the lateral sides and in the crown base of the teeth (see Material and Methods, and Fig. 1B), the abovementioned differences in centroid size might be marginally affected by differences in tooth shape at these locations (Webster and Sheets, 2010). For most specimens, these crown sides and bases include lateral cusps (between landmarks 1-13 and 21-33, Fig. 1), but also other aspects of tooth shape such as the labial notch where two successive teeth can be in contact (between landmarks 33-1, Fig. 1). Statistical analyses supported the observed sexual dimorphism of the centroid size and shape among mature specimens, as well as a visually undetected sexual dimorphism in tooth shape at hatching and juvenile

stages (Table 2 and Table 3).

We generated developmental trajectories between the three ontogenetic stages at all tooth positions in order to compare the shape transitions along jaws and ontogeny. Our analyses were performed under the hypothesis of homology (equivalence between compared structures) between tooth files of different specimens, to allow the developmental comparisons of forms over the lifetime of specimens of a given sex. However, the biological support for this hypothesis is questionable as the number of tooth files is not a fixed parameter over time. In *S. stellaris*, we also observed variation in the number of tooth files between specimens of similar total length. We chose to accept this hypothesis of homology based on the fact that newly formed tooth files are generally considered to be added at the jaw distal extremity in elasmobranchs (see Smith (2003); Smith et al. (2009); Underwood et al. (2016) for sharks and Underwood et al. (2015) for batoids). However, they also might be inserted between already existing tooth files (Reif, 1976, 1980; Smith et al., 2013), which would skew the continuity of tooth file numbering over time (see Underwood et al. (2015); Smith et al. (2013) for similar remarks on batoids). Finally, we want to highlight that this homology (comparability) hypothesis is based under the assumption that the genesis of a tooth bud happens from a defined and continuous source, which is a strongly mammal-centered view of tooth morphogenesis. In contrast, tooth bud initiation in elasmobranchs is considered to happen through self-organisation of the dental lamina, the invaginated epithelial fold from which new teeth develop (Reif, 1982; Rasch et al., 2016). For all these reasons, we interpreted our results as trends along the mesio-distal axis of a jaw but never under a strict homology hypothesis that would allow the comparison of a single given file between specimens, to the exception of the developmental trajectory analyses that necessitate a one-to-one comparison.

Over the time of sexual maturation, the juvenile-to-mature tooth shape developmental trajectories diverged between males and females at all tooth positions. In both sexes, these juvenile-to-mature developmental trajectories differed from the hatchling-to-juvenile ones (Tables 4 and 5). However, this deviation is increased in mature males ("angle cor" values are higher in males than in females in Tables 4 and 5). In males, mature tooth morphogenesis is characterized by an elongation of the main cusp and a reduction of the number of accessory cusps, generating unicuspid to tricuspid teeth similar to hatchling ones (Fig. 2 and 3). In contrast, mature female tooth shape patterns resemble those of juveniles although the most distal teeth of mature females can reach a maximum of six accessory cusps (Fig. 2 and 3). As a conclusion, during sexual maturation, all tooth files in *S. stellaris* are affected by a slighter (females) or stronger (males) modification of developmental trajectories, compared to their hatchling-to-juvenile trajectories.

On the one hand, it is tempting to speculate on dietary differences between sexes that would correlate with morphological differences in teeth. It was reported that *S. stellaris* juvenile and mature specimens mostly feed on cephalopods and, to a lesser extent, on teleosts and crustaceans (Capapé, 1975). Juvenile females were reported to feed more on crustaceans than males and mature females (Capapé, 1975). These observations do not fit with any of the morphological shifts in tooth shape described in this study, so we cannot discuss any putative link between *S. stellaris* trophic ecology and tooth shape variation. On the other hand, the gynandric heterodonty of mature *S. stellaris* is consistent with reports on the role of teeth during copulation in elasmobranchs (Springer, 1967; McEachran, 1977; Kajiura and Tricas, 1996; Pratt, Jr. and Carrier, 2001; Gutteridge and Bennett, 2014). The increased main cusp height of mature male teeth might indeed enhance gripping, as compared to teeth with more accessory cusps and smaller main cusp. However, this remains speculative as there is no experimental data on comparative gripping efficiency for shark teeth, only a few studies that compared flat *versus* cuspidate teeth in batoids (Kajiura and Tricas, 1996; Gutteridge and Bennett, 2014).

4.3 | Developmental cues linked to tooth development plasticity

Our analyses highlight features linked to tooth developmental plasticity in several ontogenetic dimensions. The notion of developmental plasticity classically refers to the building of distinct phenotypes from the expression of a same genome in different environments (Moczek, 2015). Here, we want to use a modified version of this concept and apply it to tooth shape variation: (i) of different teeth at the intra-individual level and (ii) of comparable teeth between successive ontogenetic stages. First, the intra-individual variation points to developmental plasticity which is here dependent on the mesio-distal position of the tooth bud, and which we could name "positional developmental plasticity". Second, the comparison between different ontogenetic stages —although an extrapolation of a situation with constant genome— questions developmental plasticity in the temporal dimension, assuming comparable tooth files between successive ontogenetic stages. We name this process "successive developmental plasticity", generated through tooth successional replacement. Here we have quantified a peculiarity of successive developmental plasticity: the divergence of its developmental trajectory between males and females during sexual maturation.

From these observations, we want to speculate on the potential developmental mechanisms that might generate these developmental plasticities, considering the physical and molecular cues acting on tooth bud growth within the dental lamina. To our knowledge, there are very scarce genetic data available on tooth morphogenesis in *S. stellaris* (Rasch et al., 2016) but gene regulatory networks involved in elasmobranch tooth development have been investigated in *S. canicula*. The expression of classical developmental genes was characterized in tooth buds (Debiais-Thibaud et al., 2011, 2015; Martin et al., 2016; Rasch et al., 2016), including the well-known signaling factor *Shh* that acts as both a tooth bud initiation signal and a proliferation signal during tooth morphogenesis (Berio and Debiais-Thibaud, 2019; Hosoya et al., 2020). Data on the physical features that could constrain tooth bud growth within the dental lamina are even scarcer although previous studies on mammals emphasized that a modification of the tooth bud physical environment can modify the final shape of a tooth (Renvoisé et al., 2017). Several observations of the jaw morphology may still help discuss how these physical constraints can be linked to tooth development. Of course, these genetic and physical cues acting on tooth development should not be considered as acting independently of one another on tooth development: it is likely that developmental signaling pathways impact morphogenesis by modifying physical parameters at the cellular level, while geometrical and physical constraints at the jaw cartilage or dental lamina levels can induce differential diffusion of molecules (Salazar-Ciudad, 2008; Renvoisé et al., 2017; Calamari et al., 2018). The parameters of this complex system that may be relevant for specific aspects of tooth morphology and its variational properties in time or space are essentially unknown. However, from our results in *S. stellaris*, we wish to draw three main discussion points on the putative sources of: (1) mesio-distal patterning, (2) asymmetry, and (3) gynandric heterodonty.

(1) Sources of the mesio-distal patterning. The graded variation of cusp-crown ratio is a shared feature of all ontogenetic stages and both jaws: this observation suggests the occurrence of a graded signal along the mesio-distal axis of a jaw at all developmental stages. This signal may be of two non-mutually exclusive origins: a gradient of physical constraints, and a gradient of molecular signals along the jaw.

Very little is known on the potential variation of the shape, thickness, and curvature of the dental lamina at any developmental stage. However, previous observations of catshark jaws showed that hatchling tooth buds develop very close to the Meckel's cartilage surface (observations in *S. canicula* in Debiais-Thibaud et al. (2015)), suggesting the gradient of dental lamina invagination is weak or nonexistent at this stage, contrary to older specimens whose dental lamina is more deeply invaginated. Therefore, the physical constraints on the dental lamina do not seem to explain the observed gradients of cusp-crown ratios. The overall jaw geometry may also be considered as another potential driver of the mesio-distal

patterning. As for the dental lamina, its effects on the mesio-distal patterning may however be non-linear: the sexually dimorphic heads in mature scyliorhinids would also affect the shape of jaw cartilages (Ellis and Shackley, 1995; Soares, 2019; Soares and Carvalho, 2019). This would suggest a sexual dimorphism in the gradient of cusp-crown ratio by affecting differently the labial-lingual local curvature of the dental lamina where the tooth buds develop. However, this is not obvious from our observations, although mature males tend to have a higher cusp-crown ratio in Meckelian teeth than females do, and compare best to juveniles in that respect.

On the other hand, the mesio-distal patterning of jaws by developmental genes was demonstrated in model organisms (Van Otterloo et al., 2018) and molecular signaling is known to generate the mesio-distal gradient in tooth morphology in mouse (reviewed in Cobourne and Sharpe (2003)). The genes involved in jaw patterning and tooth morphogenesis of mammals are also expressed in *S. canicula* (Debiais-Thibaud et al., 2013, 2015; Rasch et al., 2016). Yet, there is no available empirical evidence about how this signaling gradient may change during the ontogeny of scyliorhinids and whether it does correlate with the cusp-crown ratio gradient.

(2) Sources of asymmetry. The first generation of tooth buds in embryos or just hatched specimens of *S. canicula* develops very close to the surface of the jaw epithelium, within a superficial dental lamina (Debiais-Thibaud et al., 2011, 2015; Rasch et al., 2016). In addition, given the topology of the jaw symphysis (without underlying cartilage), we speculate that the situation is similar for symphyseal teeth. We therefore consider the possibility of tooth asymmetry as being correlated with the depth and topology of the dental lamina invagination. Some of our preliminary tests on modeling tooth development in sharks suggest that the mechanical stresses exerted on a tooth bud by the surrounding tissues (the dental lamina and the underlying cartilage) may be key to breaking the symmetry of the tooth morphology. We speculate that the deeper the dental lamina, the higher the likelihood of an asymmetry in the boundary conditions of the growing tooth bud reflecting into its final shape.

(3)Sources of gynandric heterodonty. Sex-related tooth shape dimorphism is visually detectable only in mature specimens. This dimorphism stands strongly in the relative size of the main cusp *versus* accessory cusps (higher in males), and in the number of accessory cusps (higher in females). Previous studies and modeling of mammalian tooth morphogenesis have recovered patterns of covariation between main cusp sharpness and the number and spacing of accessory cusps (Jernvall, 2000; Salazar-Ciudad and Jernvall, 2010). Although highly speculative to infer mammalian developmental patterns to sharks, the 2D-tooth shapes computed in this case study are very similar to the *S. stellaris* lateral teeth (especially those of the ringed seal *Phoca hispida*) (Salazar-Ciudad and Jernvall, 2010). In this case study, the authors have interpreted the observed relationship between the height of the main cusp and the height of accessory cusps as a product of the enamel knot signaling center spacing: the closer the secondary enamels knots as compared to the primary enamel knot, the higher and the more blunt the accessory cusps (Jernvall, 2000; Salazar-Ciudad and Jernvall, 2010). Conversely, when the distance between primary and secondary enamel knots is greater, sharper teeth with fewer and smaller accessory cusps develop (Jernvall, 2000; Salazar-Ciudad and Jernvall, 2010). The successive activation of enamel knots and their spacing is strongly regulated by the diffusion rate of signaling molecules such as Shh and Fgfs (Thesleff and Mikkola, 2002; Du et al., 2017). Another developmental parameter in which variation was associated with this shape relationship is epithelial growth rate (Salazar-Ciudad and Jernvall, 2010), e.g., the rate of cell division in the tooth bud that is growing from the dental lamina. Finally, the dental lamina characteristics (acting on diffusion rates and cell division rate) might exhibit sexual dimorphism, as a consequence of sexually dimorphic head dimensions in Scyliorhinidae (Ellis and Shackley, 1995; Soares, 2019). The longer and narrower jaw in males compared to females at mature stage is actually a recurrent feature in elasmobranchs and gives support to this hypothesis (Ellis and Shackley, 1995; Braccini and Chiaramonte, 2002; Erdogan et al., 2004; Geniz et al., 2007; Soares et al., 2016; Soares, 2019). Labial curva-

ture of the jaw cartilages may then impact the physical constraints on dental lamina. A second hypothetical source, which might interact with the previous one, is based on the sex-hormone dependence of the molecular signalisation involved in tooth bud growth. This is supported by previous identification of a sex-hormone dependency for *Shh* expression in vertebrates, including elasmobranchs (Ogino et al., 2004; Chew et al., 2014; O'Shaughnessy et al., 2015). Gene regulatory networks involved in elasmobranch tooth development have been most extensively investigated in *S. canicula*, where the expression of classical developmental genes was characterized (Debiais-Thibaud et al., 2011, 2015; Martin et al., 2016; Rasch et al., 2016). If the situation in *S. stellaris* is comparable to what was observed in *S. canicula*, then a modification of balance between developmental genes (e.g., *Shh*) under the reception of sex-hormone signals in mature specimens could modify the balance between cell proliferation and differentiation that impacts the final shape of a tooth.

As discussed here, a variety of hypothetical physical and molecular factors might be involved in the generation of tooth shape plasticity in elasmobranchs. To test these influences, morpho-anatomical and functional studies are still necessary although they are difficult to realize in non-model and threatened species such as most elasmobranchs. We expect that our extensive description of the actual tooth form diversity in *S. stellaris* will help to orientate the hypotheses to be further tested to identify the sources of heterodonty in elasmobranchs.

4.4 | Conclusion

Teeth are involved in two main functions in elasmobranchs: feeding and reproduction. Although ontogenetic shifts in tooth morphologies have been reported in different shark orders, very few studies focused on the changes from an embryonic to a mature dentition in males and females separately. Here we gave a description of the wide, natural, and intraspecific variation of tooth shapes in *S. stellaris*. We detailed the tooth form transitions between three ontogenetic stages and focused on: (i) graded variation of several morphometric parameters along the mesio-distal axis of a jaw, only starting during the juvenile stage and on (ii) gynandric heterodonty at mature stage generated by a stronger change in developmental trajectory for males (unicuspid to tricuspid teeth) than for females (addition of lateral cusps). We hope that the detailed morphospaces we provide here for *S. stellaris* teeth will be extended in an interspecific framework to challenge hypotheses on the developmental mechanisms that generate the known elasmobranch tooth shape diversity.

5 | ACKNOWLEDGEMENTS

We are indebted to Sylvain Adnet, Henri Cappetta, Guillaume Guinot, and Suzanne Jiquel for giving access to the collections (University of Montpellier). We also thank Sophie Germain-Pigno from the Aquarium du Cap d'Agde for providing fresh specimens, Sabrina Renaud for her advices on geometric morphometrics, and Yann Bayle, Julien Claude, Guillaume Guinot, and Roland Zimm for insightful proofreading. We acknowledge the contribution of SFR Biosciences (UMS3444/CNRS, US8/Inserm, ENS de Lyon, UCBL) facilities: AniRA-ImmOs (Mathilde Bouchet-Combe) and the contribution of MRI platform, member of the national infrastructure France-BioImaging supported by the French National Research Agency (ANR-10-INBS-04, "Investments for the future"), the labex CEMEB (ANR-10-LABX-0004) and NUMEV (ANR-10-LABX-0020) (Renaud Lebrun). The authors declare no conflict of interest. The datasets generated and analyzed in the current study are not publicly available due to ongoing other project but are available from the corresponding author on reasonable request.

6 | AUTHOR'S CONTRIBUTIONS

FB generated and analyzed the data; FB and AE designed the statistical analyses; FB, NG and MDT designed the experimental setup; FB and MDT drafted the manuscript.

References

Adams, D. C. and Otárola-Castillo, E. (2013) geomorph: an R package for the collection and analysis of geometric morphometric shape data. *Methods in Ecology and Evolution*, **4**, 393–399.

Bazzi, M., Kear, B. P., Blom, H., Ahlberg, P. E. and Campione, N. E. (2018) Static dental disparity and morphological turnover in sharks across the end-Cretaceous mass extinction. *Current Biology*, **28**, 2607–2615.e3.

Berio, F. and Bayle, Y. (2020) Scyland3D: Processing 3D landmarks. *Journal of Open Source Software*, **5**, 1262.

Berio, F. and Debiais-Thibaud, M. (2019) Evolutionary developmental genetics of teeth and odontodes in jawed vertebrates: a perspective from the study of elasmobranchs. *Journal of Fish Biology*.

Bookstein, F. L. (1991) *Morphometric tools for landmark data: geometry and biology*. Cambridge: Cambridge University Press.

— (1997) Landmark methods for forms without landmarks: morphometrics of group differences in outline shape. *Medical Image Analysis*, **1**, 225–243.

Braccini, J. M. and Chiaramonte, G. E. (2002) Intraspecific variation in the external morphology of the sand skate. *Journal of Fish Biology*, **61**, 959–972.

Brough, J. (1937) On certain Secondary Sexual Characters in the Common Dogfish (*Scyliorhinus caniculus*). *Journal of Zoology*, **107**, 217–223.

Calamari, Z. T., Hu, J. K.-H. and Klein, O. D. (2018) Tissue mechanical forces and evolutionary developmental changes act through space and time to shape tooth morphology and function. *BioEssays*, **40**, 1800140.

Capapé, C. (1975) Contribution à la biologie des Scyliorhinidae des côtes tunisiennes. IV *Scyliorhinus stellaris* (Linné, 1758). Régime alimentaire. *Archives de l'Institut Pasteur de Tunis*, **52**, 383–394.

Cappetta, H. (1986) Types dentaires adaptatifs chez les sélaciens actuels et post-paléozoïques. *Palaeovertebrata*, **16**, 57–76.

— (2012) *Handbook of Paleoichthyology, Vol 3E: Chondrichthyes - Mesozoic and Cenozoic Elasmobranchii: Teeth*. Munich: Verlag Dr. Friedrich Pfeil.

Chew, K., Pask, A., Hickford, D., Shaw, G. and Renfree, M. (2014) A dual role for SHH during phallus development in a marsupial. *Sexual Development*, **8**, 166–177.

Cobourne, M. T. and Sharpe, P. T. (2003) Tooth and jaw: molecular mechanisms of patterning in the first branchial arch. *Archives of Oral Biology*, **48**, 1–14.

Coolen, M., Menuet, A., Chassoux, D., Compagnucci, C., Henry, S., Lévèque, L., Da Silva, C., Gavory, F., Samain, S., Wincker, P., Thermes, C., D'Aubenton-Carafa, Y., Rodriguez-Moldes, I., Naylor, G., Depew, M., Sourdaine, P. and Mazan, S. (2008) The dogfish *Scyliorhinus canicula*: A reference in jawed vertebrates. *CSH protocols*, **2008**, pdb.emo111.

Correia, J. P. (1999) Tooth loss rate from two captive sandtiger sharks (*Carcharias taurus*). *Zoo Biology*, **18**, 313–317.

Cullen, J. A. and Marshall, C. D. (2019) Do sharks exhibit heterodonty by tooth position and over ontogeny? A comparison using elliptic Fourier analysis. *Journal of Morphology*, **280**, 687–700.

de Sousa Rangel, B., Santander-Neto, J., Rici, R. E. G. and Lessa, R. (2016) Dental sexual dimorphism and morphology of *Urotrygon microphthalmum*. *Zoomorphology*, **135**, 367–374.

Debiais-Thibaud, M., Chiori, R., Enault, S., Oulion, S., Germon, I., Martinand-Mari, C., Casane, D. and Borday-Birraux, V. (2015) Tooth and scale morphogenesis in shark: an alternative process to the mammalian enamel knot system. *BMC Evolutionary Biology*, **15**, 292.

Debiais-Thibaud, M., Metcalfe, C. J., Pollack, J., Germon, I., Ekker, M., Depew, M., Laurenti, P., Borday-Birraux, V. and Casane, D. (2013) Heterogeneous Conservation of *Dlx* Paralog Co-Expression in Jawed Vertebrates. *PLoS ONE*, **8**, e68182.

Debiais-Thibaud, M., Oulion, S., Bourrat, F., Laurenti, P., Casane, D. and Borday-Birraux, V. (2011) The homology of odontodes in gnathostomes: insights from Dlx gene expression in the dogfish, *Scyliorhinus canicula*. *BMC Evolutionary Biology*, **11**, 307.

Du, W., Hu, J. K. H., Du, W. and Klein, O. D. (2017) Lineage tracing of epithelial cells in developing teeth reveals two strategies for building signaling centers. *Journal of Biological Chemistry*, **292**, 15062–15069.

Ellis, J. R. and Shackley, S. E. (1995) Ontogenic changes and sexual dimorphism in the head, mouth and teeth of the lesser spotted dogfish. *Journal of Fish Biology*, **47**, 155–164.

Erdogan, Z., Koc, H., Cakir, T., Nerlović, V. and Dulčić, J. (2004) Sexual dimorphism in the small-spotted catshark *Scyliorhinus canicula* from the Edremit Bay (Turkey). *Series Historia Naturalis*, **14**, 165–170.

Feduccia, A. and Slaughter, B. H. (1974) Sexual dimorphism in skates (Rajidae) and its possible role in differential niche utilization. *Evolution*, **8**, 164–168.

Fischer, W., Bauchot, M.-L. and Schneider, M. (1987) Fiches FAO d'identification des espèces pour les besoins de la pêche (Révision 1). Méditerranée et Mer Noire. Zone de pêche 37. Vertébrés. *FAO*, **2**, 761–1530.

Frazzetta, T. H. (1988) The mechanics of cutting and the form of shark teeth (Chondrichthyes, Elasmobranchii). *Zoomorphology*, **108**, 93–107.

French, G. C. A., Stürup, M., Rizzuto, S., van Wyk, J. H., Edwards, D., Dolan, R. W., Wintner, S. P., Towner, A. V. and Hughes, W. O. H. (2017) The tooth, the whole tooth and nothing but the tooth: tooth shape and ontogenetic shift dynamics in the white shark *Carcharodon carcharias*. *Journal of Fish Biology*, **91**, 1032–1047.

Fruciano, C. (2016) Measurement error in geometric morphometrics. *Development Genes and Evolution*, **226**, 139–158.

Geniz, J., Nishizaki, O. and Perez, J. (2007) Morphological variation and sexual dimorphism in the California skate, *Raja inornata* Jordan and Gilbert, 1881 from the Gulf of California, Mexico. *Zootaxa*, **1545**, 1–16.

Gosztonyi, A. E. (1973) About sexual and secondary dimorphism of *Halaelurus bivius* (Muller & Henle, 1841) Garman 1913 (Elasmobranchii, Scyliorhinidae) in Patagonian-Fueguinas waters. *Physis A*, **32**, 317–323.

Gottfried, M. D. and Francis, M. P. (1996) Developmental changes in white shark tooth morphology: implications for studies on fossil sharks. *Journal of Vertebrate Paleontology*, **16**.

Gutteridge, A. N. and Bennett, M. B. (2014) Functional implications of ontogenetically and sexually dimorphic dentition in the eastern shovelnose ray, *Aptychotrema rostrata*. *The Journal of experimental biology*, **217**, 192–200.

Hale, L. F. and Lowe, C. G. (2008) Age and growth of the round stingray *Urobatis halleri* at Seal Beach, California. *Journal of Fish Biology*, **73**, 510–523.

Heisler, N. and Neumann, P. (1980) The role of physicochemical buffering and of bicarbonate transfer processes in intracellular pH regulation in response to changes of temperature in the larger spotted dogfish (*Scyliorhinus stellaris*). *Journal of Experimental Biology*, **85**, 99–110.

Herman, J., Hovestadt-Euler, M. and Hovestadt, D. C. (1990) Contributions to the study of the comparative morphology of teeth and other relevant ichthyodorulites in living supraspecific taxa of Chondrichthyan fishes. Part A: Selachii. No. 2b: Order: Carcharhiniformes - Family: Scyliorhinidae. *Bulletin de l'Institut Royal des Sciences Naturelles de Belgique*, **60**, 181–230.

Hosoya, A., Shalehin, N., Takebe, H., Shimo, T. and Irie, K. (2020) Sonic Hedgehog signaling and tooth development. *International Journal of Molecular Sciences*, **21**, 1587.

Iglésias, S. P., Lecointre, G. and Sellos, D. Y. (2005) Extensive paraphylies within sharks of the order Carcharhiniformes inferred from nuclear and mitochondrial genes. *Molecular Phylogenetics and Evolution*, **34**, 569–583.

Jernvall, J. (2000) Linking development with generation of novelty in mammalian teeth. *Proceedings of the National Academy of Sciences of the United States of America*, **97**, 2641–2645.

Kajiura, S. N. and Tricas, T. C. (1996) Seasonal dynamics of dental sexual dimorphism in the Atlantic stingray *Dasyatis sabina*. *Journal of Experimental Biology*, **199**, 2297–2306.

Litvinov, F. F. and Laptikhovsky, V. V. (2005) Methods of investigations of shark heterodonty and dental formulae's variability with the blue shark, *Prionace glauca* taken as an example. In *ICES CM*, 15.

Lucifora, L. O., Menni, R. C. and Escalante, A. H. (2001) Analysis of dental insertion angles in the sand tiger shark, *Carcharias taurus* (Chondrichthyes: Lamniformes). *Cybium*, **25**, 23–31.

Luer, C. A., Blum, P. C. and Gilbert, P. W. (1990) Rate of tooth replacement in the nurse shark, *Ginglymostoma cirratum*. *Copeia*, **1990**, 182–191.

Marramà, G. and Kriwet, J. (2017) Principal component and discriminant analyses as powerful tools to support taxonomic identification and their use for functional and phylogenetic signal detection of isolated fossil shark teeth. *PLoS ONE*, **12**, e0188806.

Martin, K., Rasch, L. and Cooper, R. (2016) Sox2+ progenitors in sharks link taste development with the evolution of regenerative teeth from denticles. *PNAS*, **113**, 14769–14774.

McCourt, R. and Kerstitch, A. (1980) Mating behavior and sexual dimorphism in dentition in the stingray, *Urolophus concentricus*, from the Gulf of California. *Copeia*, **1980**, 900–901.

McEachran, J. D. (1977) Reply to "Sexual dimorphism in skates (Rajidae)". *Evolution*, **31**, 218–220.

Meredith Smith, M., Underwood, C., Clark, B., Kriwet, J. and Johanson, Z. (2018) Development and evolution of tooth renewal in neoselachian sharks as a model for transformation in chondrichthyan dentitions. *Journal of Anatomy*, **232**, 891–907.

Moczek, A. P. (2015) Developmental plasticity and evolution—*quo vadis*? *Heredity*, **115**, 302–305.

Motta, P. J. and Wilga, C. D. (2001) Advances in the study of feeding behaviors, mechanisms, and mechanics of sharks. In *The behavior and sensory biology of elasmobranch fishes: an anthology in memory of Donald Richard Nelson*, 131–156. Dordrecht: Springer.

Moyer, J. K. and Bemis, W. E. (2016) Tooth microstructure and replacement in the gulper shark, *Centrophorus granulosus* (Squaliformes: Centrophoridae). *Copeia*, **104**, 529–538.

Mullin, S. K. and Taylor, P. J. (2002) The effects of parallax on geometric morphometric data. *Computers in Biology and Medicine*, **32**, 455–464.

Musa, S. M., Czachur, M. V. and Shiels, H. A. (2018) Oviparous elasmobranch development inside the egg case in 7 key stages. *PLoS ONE*, **13**, e0206984.

Ogino, Y., Katoh, H. and Yamada, G. (2004) Androgen dependent development of a modified anal fin, gonopodium, as a model to understand the mechanism of secondary sexual character expression in vertebrates. *FEBS Letters*, **575**, 119–126.

O'Shaughnessy, K. L., Dahn, R. D. and Cohn, M. J. (2015) Molecular development of chondrichthyan claspers and the evolution of copulatory organs. *Nature Communications*, **6**, 6698.

Piiper, J., Meyer, M., Worth, H. and Willmer, H. (1977) Respiration and circulation during swimming activity in the dogfish *Scyliorhinus stellaris*. *Respiration Physiology*, **30**, 221–239.

Powter, D. M., Gladstone, W. and Platell, M. (2010) The influence of sex and maturity on the diet, mouth morphology and dentition of the Port Jackson shark, *Heterodontus portusjacksoni*. *Marine and Freshwater Research*, **61**, 74.

Pratt, Jr., H. L. and Carrier, J. C. (2001) A Review of Elasmobranch Reproductive Behavior with a Case Study on the Nurse Shark, *Ginglymostoma cirratum*. *Environmental Biology of Fishes*, **60**, 157–188.

Purdy, R. W. and Francis, M. P. (2007) Ontogenetic development of teeth in *Lamna nasus* (Bonnaterre, 1758) (Chondrichthyes: Lamnidae) and its implications for the study of fossil shark teeth. *Journal of Vertebrate Paleontology*, **27**, 798–810.

Rasch, L. J., Martin, K. J., Cooper, R. L., Metscher, B. D., Underwood, C. J. and Fraser, G. J. (2016) An ancient dental gene set governs development and continuous regeneration of teeth in sharks. *Developmental Biology*, **415**, 347–370.

Reif, W.-E. (1976) Morphogenesis, pattern formation and function of the dentition of *Heterodontus* (Selachii). *Zoomorphology*, **83**, 1–47.

— (1980) A mechanism for tooth pattern reversal in sharks: the polarity switch model. *Wilhelm Roux's archives of developmental biology*, **188**, 115–122.

— (1982) Evolution of Dermal Skeleton and Dentition in Vertebrates: The Odontode Regulation Theory. In *Evolutionary Biology* (eds. M. K. Hecht, B. Wallace and G. T. Prance), chap. 7, 287–368. New York: Plenum Press.

Renvoisé, E., Kavanagh, K. D., Lazzari, V., Häkkinen, T. J., Rice, R., Pantalacci, S., Salazar-Ciudad, I. and Jernvall, J. (2017) Mechanical constraint from growing jaw facilitates mammalian dental diversity. *Proceedings of the National Academy of Sciences of the United States of America*, **114**, 9403–9408.

Salazar-Ciudad, I. (2008) Tooth morphogenesis in vivo, in vitro, and in silico. *Current Topics in Developmental Biology*, **81**, 341–371.

Salazar-Ciudad, I. and Jernvall, J. (2010) A computational model of teeth and the developmental origins of morphological variation. *Nature*, **464**, 583.

Shimada, K. (2002) Dental homologies in lamniform sharks (Chondrichthyes: Elasmobranchii). *Journal of Morphology*, **251**, 38–72.

— (2005) Phylogeny of lamniform sharks (Chondrichthyes: Elasmobranchii) and the contribution of dental characters to lamniform systematics. *Paleontological Research*, **9**, 55–72.

Smith, M. M. (2003) Vertebrate dentitions at the origin of jaws: when and how pattern evolved. *Evolution and Development*, **5**, 394–413.

Smith, M. M., Fraser, G. J., Chaplin, N., Hobbs, C. and Graham, A. (2009) Reiterative pattern of sonic hedgehog expression in the catshark dentition reveals a phylogenetic template for jawed vertebrates. *Proceedings of the Royal Society B: Biological Sciences*, **276**, 1225–33.

Smith, M. M., Johanson, Z., Underwood, C. and Diekwisch, T. G. H. (2013) Pattern formation in development of chondrichthyan dentitions: a review of an evolutionary model. *Historical Biology*, **25**, 127–142.

Snelson, F. F., Rasmussen, L., Johnson, M. R. and Hess, D. L. (1997) Serum concentrations of steroid hormones during reproduction in the Atlantic stingray, *Dasyatis sabina*. *General and Comparative Endocrinology*, **108**, 67–79.

Soares, K., Gomes, U. and De Carvalho, M. (2016) Taxonomic review of catsharks of the *Scyliorhinus haeckelii* group, with the description of a new species (Chondrichthyes: Carcharhiniformes: Scyliorhinidae). *Zootaxa*, **4066**, 501–534.

Soares, K. D. A. (2019) Sexually dimorphic body proportions in the catshark genus *Scyliorhinus* (Chondrichthyes: Carcharhiniformes: Scyliorhinidae). *Journal of Fish Biology*, **95**, 683–685.

Soares, K. D. A. and Carvalho, M. R. D. (2019) The catshark genus *Scyliorhinus* (Chondrichthyes: Carcharhiniformes: Scyliorhinidae): taxonomy, morphology and distribution. *Zootaxa*, **4601**, 1–147.

Soda, K., Slice, D. and Naylor, G. (2017) Artificial neural networks and geometric morphometric methods as a means for classification: A case-study using teeth from *Carcharhinus sp*. (Carcharhinidae). *Journal of Morphology*, **278**, 131–141.

Soldo, A., Dulcic, J., Cetinic, P. and Cetinic, P. (2000) Contribution to the study of the morphology of the teeth of the nursehound *Scyliorhinus stellaris* (Chondrichthyes: Scyliorhinidae). *Scientia Marina*, **64**, 355–356.

Springer, S. (1966) A review of western Atlantic cat sharks, Scyliorhinidae, with descriptions of a new genus and five new species. *Fishery Bulletin*, **65**, 581–624.

— (1967) Social organization of shark populations. In *Sharks, Skates and Rays* (eds. P. W. Gilbert, R. F. Mathewson and D. P. Rall), 149–174. Baltimore: Johns Hopkins Press.

— (1979) A revision of the catsharks, family Scyliorhinidae. *Tech. rep.*, US Department of Commerce.

Stalling, D., Westerhoff, M. and Hege, H. C. (2005) Amira: A highly interactive system for visual data analysis. *The visualization handbook*.

Strasburg, D. W. (1963) The diet and dentition of *Isistius brasiliensis*, with remarks on tooth replacement in other sharks. *Copeia*, 33–40.

Taniuchi, T. and Shimizu, M. (1993) Dental sexual dimorphism and food habits in the stingray *Dasyatis akajei* from Tokyo Bay, Japan. *Nippon Suisan Gakkaishi*, **59**, 53–60.

Thesleff, I. and Mikkola, M. (2002) The role of growth factors in tooth development. *International Review of Cytology*, **217**, 93–135.

Underwood, C., Johanson, Z. and Smith, M. M. (2016) Cutting blade dentitions in squaliform sharks form by modification of inherited alternate tooth ordering patterns. *Open Science*, **3**, 160385.

Underwood, C. J., Johanson, Z., Welten, M., Metscher, B., Rasch, L. J., Fraser, G. J. and Smith, M. M. (2015) Development and evolution of dentition pattern and tooth Order in the skates And rays (Batoidea; Chondrichthyes). *PLoS ONE*, **10**, e0122553.

Van Otterloo, E., Li, H., Jones, K. L. and Williams, T. (2018) AP-2α and AP-2β cooperatively orchestrate homeobox gene expression during branchial arch patterning. *Development*, **145**.

Vélez-Zuazo, X. and Agnarsson, I. (2011) Shark tales: A molecular species-level phylogeny of sharks (Selachimorpha, Chondrichthyes). *Molecular Phylogenetics and Evolution*, **58**, 207–217.

Webster, M. and Sheets, H. D. (2010) A Practical Introduction to Landmark-Based Geometric Morphometrics. *The Paleontological Society Papers*, **16**, 163–188.

Whitenack, L. B. and Gottfried, M. D. (2010) A morphometric approach for addressing tooth-based species delimitation in fossil mako sharks, *Isurus* (Elasmobranchii: Lamniformes). *Journal of Vertebrate Paleontology*, **30**, 17–25.

Wiley, D., Amenta, N., Alcantara, D., Ghosh, D., Kil, Y., Delson, E., Harcourt-Smith, W., Rohlf, F., St. John, K. and Hamann, B. (2005) Evolutionary Morphing. In *Proceedings of the IEEE International Conference on Visualization*, 431–438. Minneapolis: Institute of Electrical and Electronics Engineers (IEEE).

Wilga, C. D. and Motta, P. J. (2000) Durophagy in sharks: feeding mechanics of the hammerhead *Sphyrna tiburo*. *The Journal of Experimental Biology*, **203**, 2781–2796.

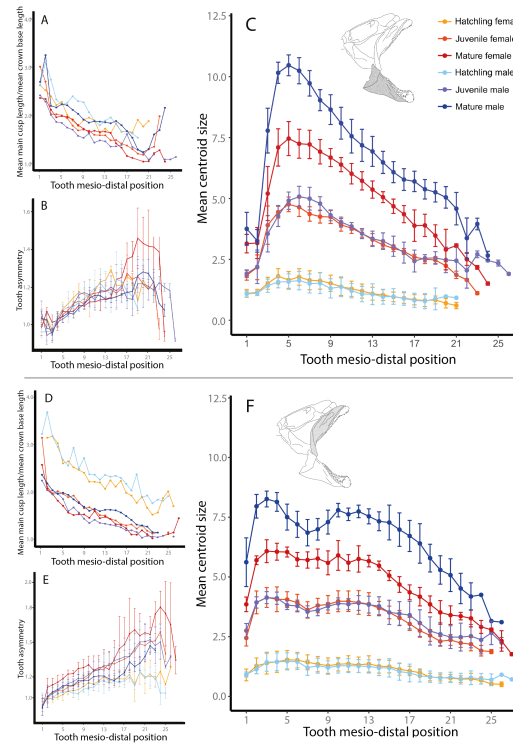

FIGURE 4 Tooth dimensions of *S. stellaris* right Meckelian and palatoquadrate teeth. A and D) Morphometric measure of the ratio between main cusp height and crown base width; B and E) Deviation to tooth bilateral symmetry: difference between the tooth tip and each crown base extremity distances. C and F) Tooth centroid sizes. At each tooth position, mean values are computed among all tooth generations (internal replicates), before being computed among all specimens. Error bars are standard deviations among replicates and specimens.

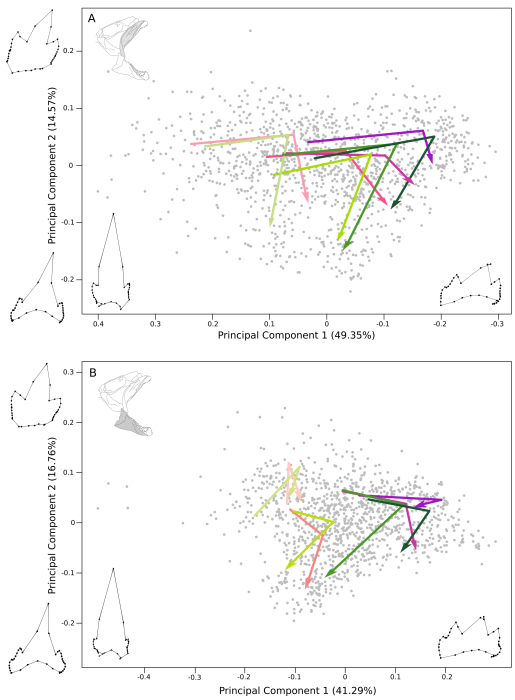

FIGURE 5 2D representation (PC1xPC2) of tooth developmental trajectories in *S. stellaris*. A) 2D trajectories for palatoquadrate tooth files 3, 10, 15 and 20; B) 2D trajectories for Meckel's tooth files 1, 5, 15, and 20. The trajectory representations are drawn between the mean shape of hatchling (starting point), juvenile, and mature (arrow tip) specimen teeth. Purple and green shades are for females and males trajectories respectively. Mesial to distal files appear in light to deep shades.

7 | SUPPLEMENTARY MATERIAL

ADDITIONAL FIGURE Tooth main cusp height and crown base width in *S. stellaris*. A) Meckelian teeth of hatchlings; B) Palatoquadrate teeth of hatchlings; C) Meckelian teeth of juveniles; D) Palatoquadrate teeth of juveniles; E) Meckelian teeth of matures; F) Palatoquadrate teeth of matures. The main cusp values are the mean lengths between the mesial-most landmark of the tooth and the main cusp tip, and the distal-most landmark of the tooth and the main cusp tip (d1-17 and d17-33). The crown base values are the lengths between the mesial-most and the distal-most landmarks on the tooth (d1-38).

ADDITIONAL TABLE 1 Developmental trajectory values within sexes for palatoquadrate teeth. Significant p-values after Benjamini & Hochberg correction are in bold. Due to the difference in total tooth file number between stages, some comparisons could not be done (NAs). -, difference; dL, delta length; HJ, hatchling-to-juvenile; JM, juvenile-to-mature.

File	Females	Males	Females	Males
	dL (JM-HJ) (p-val)	dL (JM-HJ) (p-val)	angle cor (p-val)	angle cor (p-val)
1	$-5.11e^{-2}$ ($5.40e^{-2}$)	$1.70e^{-3}$ ($9.54e^{-1}$)	1.21 (**$1.00e^{-3}$**)	1.83 (**$1.00e^{-3}$**)
2	$-4.70e^{-2}$ ($1.59e^{-1}$)	$-5.33e^{-2}$ (**$4.60e^{-2}$**)	1.76 (**$1.00e^{-3}$**)	1.99 (**$1.00e^{-3}$**)
3	$-8.42e^{-2}$ (**$3.20e^{-2}$**)	$2.08e^{-2}$ ($5.40e^{-1}$)	1.62 (**$1.00e^{-3}$**)	1.96 (**$1.00e^{-3}$**)
4	$-1.00e^{-1}$ (**$5.00e^{-3}$**)	$-5.00e^{-4}$ ($9.88e^{-1}$)	1.41 (**$1.00e^{-3}$**)	2.00 (**$1.00e^{-3}$**)
5	$-3.93e^{-2}$ ($1.77e^{-1}$)	$3.60e^{-2}$ ($2.40e^{-1}$)	1.29 (**$1.00e^{-3}$**)	2.10 (**$1.00e^{-3}$**)
6	$-5.88e^{-2}$ (**$2.60e^{-2}$**)	$1.45e^{-2}$ ($6.84e^{-1}$)	1.25 (**$1.00e^{-3}$**)	2.20 (**$1.00e^{-3}$**)
7	$-4.40e^{-2}$ ($7.10e^{-2}$)	$-2.18e^{-2}$ ($4.56e^{-1}$)	1.08 (**$1.00e^{-3}$**)	2.11 (**$1.00e^{-3}$**)
8	$-7.89e^{-2}$ (**$1.10e^{-2}$**)	$-6.10e^{-3}$ ($8.30e^{-1}$)	1.26 (**$1.00e^{-3}$**)	2.13 (**$1.00e^{-3}$**)
9	$-8.76e^{-2}$ (**$2.00e^{-3}$**)	$-2.71e^{-2}$ ($9.70e^{-1}$)	1.56 (**$1.00e^{-3}$**)	2.01 (**$1.00e^{-3}$**)
10	$-5.10e^{-2}$ ($6.10e^{-2}$)	$-2.69e^{-2}$ ($4.59e^{-1}$)	1.36 (**$1.00e^{-3}$**)	2.06 (**$1.00e^{-3}$**)
11	$-8.35e^{-2}$ (**$1.50e^{-2}$**)	$-2.70e^{-3}$ ($9.30e^{-1}$)	1.83 (**$1.00e^{-3}$**)	1.97 (**$1.00e^{-3}$**)
12	$-1.26e^{-1}$ (**$3.00e^{-3}$**)	$-1.86e^{-2}$ ($5.70e^{-1}$)	1.56 (**$2.00e^{-3}$**)	2.00 (**$1.00e^{-3}$**)
13	$-9.78e^{-2}$ (**$1.10e^{-2}$**)	$-4.97e^{-2}$ ($2.08e^{-1}$)	1.74 (**$3.00e^{-3}$**)	2.03 (**$1.00e^{-3}$**)
14	$-1.45e^{-1}$ (**$3.00e^{-3}$**)	$-1.83e^{-2}$ ($6.13e^{-1}$)	1.56 (**$1.00e^{-3}$**)	2.15 (**$1.00e^{-3}$**)
15	$-1.18e^{-1}$ (**$4.00e^{-3}$**)	$-2.78e^{-2}$ ($4.32e^{-1}$)	1.18 (**$1.00e^{-3}$**)	2.11 (**$1.00e^{-3}$**)
16	$-1.58e^{-1}$ (**$2.00e^{-3}$**)	$-2.93e^{-2}$ ($3.20e^{-1}$)	1.53 (**$1.00e^{-3}$**)	2.20 (**$1.00e^{-3}$**)
17	$-1.55e^{-1}$ (**$1.00e^{-3}$**)	$-6.93e^{-2}$ ($5.90e^{-2}$)	1.40 (**$1.00e^{-3}$**)	1.98 (**$1.00e^{-3}$**)
18	$9.58e^{-2}$ (**$2.10e^{-2}$**)	$-5.08e^{-2}$ ($1.08e^{-1}$)	$9.81e^{-1}$ (**$1.00e^{-3}$**)	2.09 (**$1.00e^{-3}$**)
19	$-1.34e^{-1}$ (**$4.00e^{-3}$**)	$-9.68e^{-2}$ (**$5.00e^{-3}$**)	$8.51e^{-1}$ (**$3.00e^{-3}$**)	2.05 (**$1.00e^{-3}$**)
20	$-1.66e^{-1}$ (**$1.00e^{-3}$**)	$-1.06e^{-1}$ (**$1.90e^{-2}$**)	1.56 (**$1.00e^{-3}$**)	2.26 (**$1.00e^{-3}$**)
21	$-1.66e^{-1}$ (**$1.00e^{-3}$**)	$-1.23e^{-1}$ (**$1.30e^{-2}$**)	1.55 (**$1.00e^{-3}$**)	2.29 (**$1.00e^{-3}$**)
22	$-1.86e^{-1}$ (**$1.00e^{-3}$**)	$-1.42e^{-1}$ (**$9.00e^{-3}$**)	1.54 (**$1.00e^{-3}$**)	2.49 (**$1.00e^{-3}$**)
23	$-1.13e^{-1}$ ($4.00e^{-2}$)	$-9.82e^{-2}$ ($1.11e^{-1}$)	1.43 (**$1.00e^{-3}$**)	2.32 (**$7.00e^{-3}$**)
24	$-1.14e^{-1}$ (**$2.50e^{-2}$**)	NA	1.45 (**$3.00e^{-3}$**)	NA
25	$-1.95e^{-1}$ (**$1.00e^{-2}$**)	NA	1.71 (**$1.20e^{-2}$**)	NA

ADDITIONAL TABLE 2 Developmental trajectory values within sexes for Meckelian teeth. Significant p-values after Benjamini & Hochberg correction are in bold. Due to the difference in total tooth file number between stages, some comparisons could not be done (NAs). -, difference; dL, delta length; HJ, hatchling-to-juvenile; JM, juvenile-to-mature.

File	Females	Males	Females	Males
	dL (JM-HJ) (p-val)	dL (JM-HJ) (p-val)	angle cor (p-val)	angle cor (p-val)
1	$4.75e^{-3}$ ($8.40e^{-1}$)	$3.22e^{-2}$ ($1.40e^{-1}$)	2.38 (**$4.00e^{-3}$**)	1.84 (**$1.00e^{-3}$**)
2	$1.23e^{-2}$ ($6.64e^{-1}$)	$1.25e^{-1}$ (**$1.00e^{-2}$**)	2.17 (**$9.00e^{-3}$**)	2.27 (**$1.00e^{-3}$**)
3	$-7.49e^{-4}$ ($9.78e^{-1}$)	$1.99e^{-2}$ ($4.35e^{-1}$)	1.82 (**$1.00e^{-3}$**)	1.99 (**$1.00e^{-3}$**)
4	$-7.83e^{-3}$ ($6.50e^{-1}$)	$8.41e^{-3}$ ($7.00e^{-1}$)	1.74 (**$1.00e^{-3}$**)	2.13 (**$1.00e^{-3}$**)
5	$-5.86e^{-3}$ ($8.00e^{-1}$)	$1.22e^{-2}$ ($5.85e^{-1}$)	1.71 (**$1.00e^{-3}$**)	2.07 (**$1.00e^{-3}$**)
6	$-3.00e^{-3}$ ($9.12e^{-1}$)	$4.08e^{-2}$ ($1.17e^{-1}$)	1.85 (**$1.00e^{-3}$**)	2.21 (**$1.00e^{-3}$**)
7	$3.85e^{-3}$ ($8.60e^{-1}$)	$1.55e^{-2}$ ($5.85e^{-1}$)	1.55 (**$1.00e^{-3}$**)	2.17 (**$1.00e^{-3}$**)
8	$-6.65e^{-3}$ ($7.65e^{-1}$)	$2.73e^{-2}$ ($3.13e^{-1}$)	1.84 (**$2.00e^{-3}$**)	2.23 (**$1.00e^{-3}$**)
9	$-4.47e^{-2}$ (**$2.30e^{-2}$**)	$1.80e^{-2}$ ($4.97e^{-1}$)	1.67 (**$1.00e^{-3}$**)	2.19 (**$1.00e^{-3}$**)
10	$-4.92e^{-2}$ (**$4.40e^{-2}$**)	$5.72e^{-2}$ ($5.40e^{-1}$)	1.56 (**$2.00e^{-3}$**)	2.04 (**$1.00e^{-3}$**)
11	$-5.60e^{-2}$ (**$1.40e^{-2}$**)	$8.30e^{-3}$ ($7.63e^{-1}$)	1.73 (**$1.00e^{-3}$**)	2.12 (**$1.00e^{-3}$**)
12	$-5.02e^{-2}$ (**$3.80e^{-2}$**)	$2.43e^{-2}$ ($3.11e^{-1}$)	1.57 (**$1.00e^{-3}$**)	2.03 (**$1.00e^{-3}$**)
13	$-6.95e^{-2}$ (**$4.00e^{-3}$**)	$1.73e^{-2}$ ($6.30e^{-1}$)	1.61 (**$1.00e^{-3}$**)	2.22 (**$2.00e^{-3}$**)
14	$-8.06e^{-2}$ (**$1.00e^{-3}$**)	$1.12e^{-3}$ ($9.77e^{-1}$)	1.59 (**$1.00e^{-3}$**)	2.19 (**$1.00e^{-3}$**)
15	$-8.27e^{-2}$ (**$8.00e^{-3}$**)	$3.86e^{-2}$ ($3.04e^{-1}$)	1.51 (**$1.00e^{-3}$**)	2.25 (**$2.00e^{-3}$**)
16	$-9.22e^{-2}$ (**$1.00e^{-3}$**)	$1.86e^{-2}$ ($5.42e^{-1}$)	1.66 (**$1.00e^{-3}$**)	2.17 (**$1.00e^{-3}$**)
17	$-1.11e^{-1}$ (**$1.00e^{-3}$**)	$4.87e^{-2}$ ($1.91e^{-1}$)	1.53 (**$3.00e^{-3}$**)	2.01 (**$1.00e^{-3}$**)
18	$-1.27e^{-1}$ (**$1.00e^{-3}$**)	$-2.11e^{-2}$ ($4.39e^{-1}$)	1.41 (**$1.00e^{-3}$**)	2.17 (**$1.00e^{-3}$**)
19	$-1.51e^{-1}$ (**$1.00e^{-3}$**)	$-4.49e^{-2}$ ($1.90e^{-1}$)	1.20 (**$1.00e^{-3}$**)	2.08 (**$1.00e^{-3}$**)
20	$-1.49e^{-1}$ (**$6.00e^{-3}$**)	NA	2.39 (**$2.00e^{-3}$**)	NA
21	$-8.47e^{-2}$ (**$1.40e^{-2}$**)	NA	1.08 (**$1.00e^{-3}$**)	NA

8 | TABLES

TABLE 1 Scanned *Scyliorhinus stellaris* specimens. etOH, 70% ethanol; F, female; Hat, hatchling stage; Juv, juvenile stage; M, male; Mat, mature stage; Mc, Meckel cartilage; Pq, palatoquadrate.

Specimen	Sex	Stage (TL, cm)	Cartilage	Preservation	Scanning resolution (μm)
100418A	F	Hat (22)	Both	etOH	13.18
100418B	F	Hat (21)	Both	etOH	13.18
100418D	F	Hat (14)	Both	etOH	8.64
100418E	M	Hat (17.5)	Both	etOH	13.00
100418F	M	Hat (14)	Both	etOH	9.41
100418G	F	Hat (14)	Both	etOH	9.41
100418H	M	Hat (17)	Both	etOH	14.26
160118B	F	Hat (17)	Both	etOH	10.88
160118C	F	Hat (17)	Both	etOH	11.16
160118D	F	Hat (17.5)	Both	etOH	11.40
160118E	M	Hat (16.5)	Both	etOH	10.51
230918A	M	Hat (24.5)	Both	etOH	10.00
000000B	F	Juv (64)	Pq	Air	16.61
000000C	M	Juv (56)	Pq	Air	16.61
UM REC0371M	M	Juv (53)	Pq	Air	15.60
UM REC0778M	M	Juv (59)	Both	Air	19.17
UM REC1068M	F	Juv (55)	Both	Air	16.56
UM REC1073M	M	Juv (60)	Both	Air	14.29
UM REC1074M	F	Juv (57)	Both	Air	18.33
UM REC1075M	F	Juv (59)	Both	Air	12.50
UM REC1076M	F	Juv (55)	Both	Air	16.00
UM REC1077M	M	Juv (59)	Both	Air	21.28
UM REC0185M	M	Mat (112)	Mc	Air	26.93
UM REC0187M	M	Mat (106)	Mc	Air	26.93
UM REC0188M	M	Mat (113)	Pq	Air	26.93
UM REC0189M	F	Mat (93)	Both	Air	26.93
UM REC0353M	F	Mat (95)	Mc	Air	18.52
UM REC1312M	M	Mat (98)	Both	Air	30.00
UM REC1496M	M	Mat (102)	Both	Air	29.75
UM REC1497M	M	Mat (105)	Both	Air	30.00
UM REC1498M	M	Mat (110)	Both	Air	30.00
UM REC1499M	F	Mat (94)	Both	Air	25.00
UM REC1500M	F	Mat (102)	Both	Air	30.00

TABLE 2 ANOVA results on centroid sizes. Significant p-values after Benjamini & Hochberg correction are in bold.

	Meckelian teeth			
	All	Hatchling	Juvenile	Mature
	F value (p-val)	F value (p-val)	F value (p-val)	F value (p-val)
Sex	2.37 ($1.26e^{-1}$)	$1.47e^{-1}$ ($7.04e^{-1}$)	$4.00e^{-2}$ ($8.42e^{-1}$)	6.33 (**$1.54e^{-2}$**)
Stage	$1.03e^{2}$ (**$< 2.00e^{-16}$**)	-	-	-
ToothMD	1.09 ($3.61e^{-1}$)	$2.43e^{1}$ (**$2.67e^{-10}$**)	$1.48e^{1}$ (**$4.69e^{-9}$**)	5.39 (**$5.77e^{-5}$**)
Sex:Stage	5.99 (**$3.24e^{-3}$**)	-	-	-
Sex:ToothMD	$2.20e^{-2}$ (1.00)	-	-	-
Stage:ToothMD	2.14 ($2.49e^{-3}$)	-	-	-
	Palatoquadrate teeth			
	All	Hatchling	Juvenile	Mature
	F value (p-val)	F value (p-val)	F value (p-val)	F value (p-val)
Sex	2.83 ($9.48e^{-2}$)	$4.52e^{-1}$ ($5.04e^{-1}$)	$1.00e^{-3}$ ($9.70e^{-1}$)	$1.48e^{1}$ (**$3.32e^{-4}$**)
Stage	$2.24e^{2}$ (**$2.00e^{-16}$**)	-	-	-
ToothMD	$8.29e^{-1}$ ($7.03e^{-1}$)	$1.91e^{1}$ (**$3.44e^{-11}$**)	$2.72e^{1}$ (**$1.33e^{-12}$**)	3.56 (**$9.37e^{-4}$**)
Sex:Stage	$1.59e^{1}$ (**$5.48e^{-7}$**)	-	-	-
Sex:ToothMD	$1.50e^{-2}$ (1.00)	-	-	-
Stage:ToothMD	1.33 ($1.28e^{-1}$)	-	-	-

TABLE 3 MANOVA results on shape data. Significant p-values after Benjamini & Hochberg correction are in bold. MD, mesio-distal.

	Meckelian teeth			
	All	Hatchling	Juvenile	Mature
	F approx (p-val)	F approx (p-val)	F approx (p-val)	F approx (p-val)
Sex	5.39 (**$6.13e^{-8}$**)	4.02 (**$9.54e^{-4}$**)	$1.86e^{1}$ (**$5.72e^{-12}$**)	$2.67e^{1}$ (**$5.39e^{-14}$**)
Stage	$3.04e^{1}$ (**$< 2.20e^{-16}$**)	-	-	-
ToothMD	1.80 (**$3.12e^{-14}$**)	1.09 ($2.36e^{-1}$)	1.50 (**$1.16e^{-4}$**)	1.03 ($4.12e^{-1}$)
Sex:Stage	$1.05e^{1}$ (**$< 2.20e^{-16}$**)	-	-	-
Sex:ToothMD	$8.73e^{-1}$ ($9.33e^{-1}$)	-	-	-
Stage:ToothMD	1.18 (**$1.02e^{-2}$**)	-	-	-
	Palatoquadrate teeth			
	All	Hatchling	Juvenile	Mature
	F approx (p-val)	F approx (p-val)	F approx (p-val)	F approx (p-val)
Sex	7.61 (**$2.67e^{-11}$**)	2.88 (**$5.37e^{-3}$**)	4.84 (**$7.58e^{-5}$**)	$5.99e^{1}$ (**$< 2.20e^{-16}$**)
Stage	$4.58e^{1}$ (**$< 2.20e^{-16}$**)	-	-	-
ToothMD	1.89 (**$3.36e^{-16}$**)	1.65 (**$2.28e^{-6}$**)	1.52 (**$9.56e^{-5}$**)	1.17 ($7.37e^{-2}$)
Sex:Stage	7.32 (**$< 2.20e^{-16}$**)	-	-	-
Sex:ToothMD	$8.63e^{-1}$ ($9.53e^{-1}$)	-	-	-
Stage:ToothMD	1.50 (**$4.16e^{-9}$**)	-	-	-

TABLE 4 Developmental trajectory values between sexes for palatoquadrate teeth. Significant p-values after Benjamini & Hochberg correction are in bold. Due to the difference in total tooth file number between stages, some comparisons could not be done (NAs). -, difference; dL, delta length; F, females; M, males.

	All stages	Juvenile to mature stage		hatchling to juvenile stage	
File	M/F shape (p-val)	dL (M-F) (p-val)	MF angle cor (p-val)	dL (M-F) (p-val)	MF angle cor (p-val)
1	$3.08e^{-1}$ ($6.10e^{-2}$)	$7.39e^{-2}$ (**$3.00e^{-3}$**)	1.21 (**$1.00e^{-3}$**)	$2.12e^{-2}$ ($4.89e^{-1}$)	$6.57e^{-1}$ ($1.20e^{-2}$)
2	$1.13e^{-1}$ ($5.90e^{-1}$)	$4.14e^{-2}$ ($9.60e^{-2}$)	1.04 (**$1.00e^{-3}$**)	$4.77e^{-2}$ ($1.97e^{-1}$)	$4.90e^{-1}$ ($3.10e^{-2}$)
3	$3.34e^{-1}$ ($3.20e^{-2}$)	$7.05e^{-2}$ (**$1.70e^{-2}$**)	$9.63e^{-1}$ (**$1.00e^{-3}$**)	$-3.45e^{-2}$ ($4.05e^{-1}$)	$3.35e^{-1}$ ($1.23e^{-1}$)
4	$3.86e^{-1}$ (**$1.40e^{-2}$**)	$6.29e^{-2}$ (**$3.40e^{-2}$**)	$9.19e^{-1}$ (**$1.00e^{-3}$**)	$-3.66e^{-2}$ ($3.64e^{-1}$)	$4.24e^{-1}$ ($2.40e^{-2}$)
5	$4.41e^{-1}$ (**$2.00e^{-3}$**)	$6.58e^{-2}$ (**$2.90e^{-2}$**)	1.05 (**$1.00e^{-3}$**)	$-9.50e^{-3}$ ($7.45e^{-1}$)	$6.44e^{-1}$ ($2.30e^{-2}$)
6	$4.95e^{-1}$ (**$1.00e^{-3}$**)	$7.13e^{-2}$ (**$1.10e^{-2}$**)	1.03 (**$1.00e^{-3}$**)	$-2.10e^{-3}$ ($9.45e^{-1}$)	$4.35e^{-1}$ ($1.90e^{-2}$)
7	$4.58e^{-1}$ (**$1.00e^{-3}$**)	$6.88e^{-2}$ (**$5.00e^{-3}$**)	1.22 (**$1.00e^{-3}$**)	$4.67e^{-2}$ ($1.44e^{-1}$)	$3.64e^{-1}$ ($1.90e^{-2}$)
8	$4.54e^{-1}$ (**$1.00e^{-3}$**)	$7.85e^{-2}$ (**$5.00e^{-3}$**)	$9.69e^{-1}$ (**$1.00e^{-3}$**)	$5.60e^{-3}$ ($8.51e^{-1}$)	$3.37e^{-1}$ ($1.07e^{-1}$)
9	$2.93e^{-1}$ ($4.60e^{-2}$)	$7.64e^{-2}$ (**$3.00e^{-3}$**)	$7.97e^{-1}$ (**$1.00e^{-3}$**)	$1.59e^{-2}$ ($6.25e^{-1}$)	$2.74e^{-1}$ ($1.17e^{-1}$)
10	$3.32e^{-1}$ (**$1.20e^{-2}$**)	$5.17e^{-2}$ ($6.60e^{-2}$)	1.04 (**$1.00e^{-3}$**)	$2.76e^{-2}$ ($3.66e^{-1}$)	$3.47e^{-1}$ ($8.30e^{-2}$)
11	$3.14e^{-1}$ ($3.50e^{-2}$)	$9.38e^{-2}$ (**$3.00e^{-3}$**)	$6.26e^{-1}$ (**$4.00e^{-3}$**)	$1.30e^{-2}$ ($7.25e^{-1}$)	$3.07e^{-1}$ ($2.20e^{-2}$)
12	$4.11e^{-1}$ (**$3.00e^{-3}$**)	$1.02e^{-1}$ (**$1.00e^{-3}$**)	$8.58e^{-1}$ (**$2.00e^{-3}$**)	$-5.80e^{-3}$ ($8.75e^{-1}$)	$3.47e^{-1}$ ($1.00e^{-2}$)
13	$2.55e^{-1}$ ($1.82e^{-1}$)	$8.29e^{-2}$ (**$1.20e^{-2}$**)	$6.53e^{-1}$ (**$2.60e^{-2}$**)	$3.48e^{-2}$ ($4.18e^{-1}$)	$3.68e^{-1}$ ($1.80e^{-2}$)
14	$4.76e^{-1}$ (**$5.00e^{-3}$**)	$1.23e^{-1}$ (**$1.00e^{-3}$**)	1.06 (**$1.00e^{-3}$**)	$-3.50e^{-3}$ ($9.46e^{-1}$)	$3.59e^{-1}$ ($4.00e^{-3}$)
15	$4.85e^{-1}$ (**$1.00e^{-3}$**)	$1.25e^{-1}$ (**$2.00e^{-3}$**)	1.22 (**$1.00e^{-3}$**)	$3.48e^{-2}$ ($3.43e^{-1}$)	$3.05e^{-1}$ ($2.00e^{-2}$)
16	$4.88e^{-1}$ (**$1.00e^{-3}$**)	$1.17e^{-1}$ (**$1.00e^{-3}$**)	$8.27e^{-1}$ (**$3.00e^{-3}$**)	$-1.13e^{-2}$ ($7.59e^{-1}$)	$2.90e^{-1}$ ($2.60e^{-2}$)
17	$3.68e^{-1}$ (**$1.20e^{-2}$**)	$1.09e^{-1}$ (**$1.00e^{-3}$**)	1.15 (**$1.00e^{-3}$**)	$2.40e^{-2}$ ($5.14e^{-1}$)	$3.63e^{-1}$ ($1.20e^{-2}$)
18	$4.63e^{-1}$ (**$2.00e^{-3}$**)	$6.49e^{-2}$ (**$3.30e^{-2}$**)	1.38 (**$1.00e^{-3}$**)	$1.99e^{-2}$ ($5.33e^{-1}$)	$3.45e^{-1}$ ($6.90e^{-2}$)
19	$4.41e^{-1}$ (**$2.00e^{-3}$**)	$9.03e^{-2}$ (**$4.00e^{-3}$**)	1.58 (**$1.00e^{-3}$**)	$5.27e^{-2}$ ($2.07e^{-1}$)	$2.60e^{-1}$ ($1.18e^{-1}$)
20	$3.54e^{-1}$ (**$4.00e^{-3}$**)	$8.28e^{-2}$ (**$1.00e^{-3}$**)	1.17 (**$3.00e^{-3}$**)	$2.24e^{-2}$ ($5.34e^{-1}$)	$3.25e^{-1}$ ($3.40e^{-2}$)
21	$3.36e^{-1}$ (**$9.00e^{-3}$**)	$8.08e^{-2}$ (**$1.00e^{-3}$**)	1.08 (**$1.00e^{-3}$**)	$3.72e^{-2}$ ($2.54e^{-1}$)	$2.26e^{-1}$ ($7.50e^{-2}$)
22	$3.31e^{-1}$ ($3.90e^{-2}$)	$4.88e^{-2}$ (**$1.90e^{-2}$**)	1.25 (**$9.00e^{-3}$**)	$4.20e^{-3}$ ($9.16e^{-1}$)	$2.95e^{-1}$ ($2.50e^{-2}$)
23	$3.77e^{-1}$ ($1.14e^{-1}$)	$3.16e^{-2}$ ($2.44e^{-1}$)	1.37 (**$2.00e^{-3}$**)	$1.71e^{-2}$ ($7.15e^{-1}$)	$3.29e^{-1}$ ($2.00e^{-2}$)
24	NA	NA	NA	$2.44e^{-2}$ ($5.69e^{-1}$)	$5.88e^{-1}$ ($4.00e^{-3}$)
25	NA	NA	NA	$2.63e^{-2}$ ($7.13e^{-1}$)	$8.04e^{-1}$ ($2.20e^{-2}$)

TABLE 5 Developmental trajectory values between sexes for Meckelian teeth. Significant p-values after Benjamini & Hochberg correction are in bold. Due to the difference in total tooth file number between stages, some comparisons could not be done (NAs). -, difference; dL, delta length; F, females; M, males.

	All stages	Juvenile to mature stage		hatchling to juvenile stage	
File	M/F shape (p-val)	dL (M-F) (p-val)	MF angle cor (p-val)	dL (M-F) (p-val)	MF angle cor (p-val)
1	$3.30e^{-1}$ ($7.20e^{-2}$)	$4.88e^{-2}$ (**$2.10e^{-2}$**)	1.14 (**$1.00e^{-3}$**)	$2.14e^{-2}$ ($3.11e^{-1}$)	$9.65e^{-1}$ ($1.10e^{-2}$)
2	$3.11e^{-1}$ ($2.56e^{-1}$)	$1.54e^{-1}$ (**$1.00e^{-3}$**)	1.49 (**$1.00e^{-3}$**)	$4.04e^{-2}$ ($1.04e^{-1}$)	$9.16e^{-1}$ ($3.00e^{-3}$)
3	$1.11e^{-1}$ ($7.19e^{-1}$)	$5.95e^{-2}$ (**$8.00e^{-3}$**)	$7.61e^{-1}$ (**$3.00e^{-3}$**)	$3.88e^{-2}$ ($1.86e^{-1}$)	$7.27e^{-1}$ ($5.00e^{-3}$)
4	$2.07e^{-1}$ ($1.19e^{-1}$)	$5.46e^{-2}$ (**$3.40e^{-2}$**)	$5.05e^{-1}$ (**$2.40e^{-2}$**)	$5.40e^{-2}$ ($6.00e^{-3}$)	$7.63e^{-1}$ (**$1.00e^{-3}$**)
5	$1.98e^{-1}$ ($2.19e^{-1}$)	$5.20e^{-2}$ ($9.70e^{-2}$)	$7.55e^{-1}$ (**$1.30e^{-2}$**)	$3.39e^{-2}$ ($1.02e^{-1}$)	$6.32e^{-1}$ ($1.70e^{-2}$)
6	$2.44e^{-1}$ ($1.54e^{-1}$)	$8.06e^{-2}$ (**$1.40e^{-2}$**)	$6.96e^{-1}$ (**$8.00e^{-3}$**)	$3.71e^{-2}$ ($1.54e^{-1}$)	$6.41e^{-1}$ ($1.50e^{-2}$)
7	$3.14e^{-1}$ ($5.20e^{-2}$)	$6.35e^{-2}$ (**$3.00e^{-2}$**)	$7.71e^{-1}$ (**$3.10e^{-2}$**)	$5.19e^{-2}$ ($1.07e^{-1}$)	$6.76e^{-1}$ ($2.90e^{-2}$)
8	$2.52e^{-1}$ ($1.78e^{-1}$)	$9.04e^{-2}$ (**$4.00e^{-3}$**)	$7.58e^{-1}$ (**$1.70e^{-2}$**)	$5.65e^{-2}$ ($2.10e^{-2}$)	$7.69e^{-1}$ ($8.00e^{-3}$)
9	$4.01e^{-1}$ (**$1.60e^{-2}$**)	$1.01e^{-1}$ (**$1.00e^{-3}$**)	$8.20e^{-1}$ (**$1.00e^{-2}$**)	$3.85e^{-2}$ ($2.20e^{-1}$)	$6.42e^{-1}$ ($1.10e^{-2}$)
10	$4.82e^{-1}$ (**$6.00e^{-3}$**)	$1.15e^{-1}$ (**$1.00e^{-3}$**)	$9.85e^{-1}$ (**$3.00e^{-3}$**)	$8.46e^{-3}$ ($7.74e^{-1}$)	$5.45e^{-1}$ ($5.70e^{-2}$)
11	$3.76e^{-1}$ (**$1.40e^{-2}$**)	$1.03e^{-1}$ (**$1.00e^{-3}$**)	$9.61e^{-1}$ (**$4.00e^{-3}$**)	$3.86e^{-2}$ ($1.84e^{-1}$)	$4.83e^{-1}$ ($2.10e^{-2}$)
12	$3.88e^{-1}$ (**$1.60e^{-2}$**)	$1.05e^{-1}$ (**$1.00e^{-3}$**)	$8.80e^{-1}$ (**$2.00e^{-3}$**)	$3.01e^{-2}$ ($2.92e^{-1}$)	$4.74e^{-1}$ ($5.10e^{-2}$)
13	$4.97e^{-1}$ (**$2.00e^{-3}$**)	$1.23e^{-1}$ (**$1.00e^{-3}$**)	$8.04e^{-1}$ (**$1.00e^{-3}$**)	$3.61e^{-2}$ ($2.20e^{-1}$)	$3.94e^{-1}$ ($1.00e^{-1}$)
14	$4.72e^{-1}$ (**$4.00e^{-3}$**)	$1.43e^{-1}$ (**$1.00e^{-3}$**)	1.02 (**$1.00e^{-3}$**)	$6.14e^{-2}$ ($4.20e^{-2}$)	$4.14e^{-1}$ ($1.20e^{-2}$)
15	$5.51e^{-1}$ (**$2.00e^{-3}$**)	$1.33e^{-1}$ (**$1.00e^{-3}$**)	1.02 (**$1.00e^{-3}$**)	$1.19e^{-2}$ ($7.40e^{-1}$)	$2.78e^{-1}$ ($2.43e^{-1}$)
16	$5.11e^{-1}$ (**$2.00e^{-3}$**)	$1.07e^{-1}$ (**$1.00e^{-3}$**)	1.01 (**$1.00e^{-3}$**)	$-3.27e^{-3}$ ($9.17e^{-1}$)	$3.68e^{-1}$ ($1.39e^{-1}$)
17	$5.99e^{-1}$ (**$2.00e^{-3}$**)	$1.15e^{-1}$ (**$1.00e^{-3}$**)	1.17 (**$3.00e^{-3}$**)	$-4.49e^{-2}$ ($2.42e^{-1}$)	$7.78e^{-1}$ ($2.90e^{-2}$)
18	$5.02e^{-1}$ (**$1.00e^{-3}$**)	$9.26e^{-2}$ (**$6.00e^{-3}$**)	1.23 (**$5.00e^{-3}$**)	$-1.33e^{-2}$ ($7.28e^{-1}$)	$3.75e^{-1}$ ($1.42e^{-1}$)
19	$4.43e^{-1}$ (**$1.00e^{-3}$**)	$5.94e^{-2}$ (**$1.50e^{-2}$**)	1.47 (**$3.00e^{-3}$**)	$-4.71e^{-2}$ ($1.78e^{-1}$)	$3.93e^{-1}$ ($2.30e^{-2}$)
20	NA	$4.02e^{-2}$ ($1.42e^{-1}$)	$9.81e^{-1}$ ($1.09e^{-1}$)	NA	NA
21	NA	$4.10e^{-3}$ ($8.47e^{-1}$)	1.57 (**$1.00e^{-3}$**)	NA	NA
22	NA	$7.71e^{-2}$ ($5.40e^{-2}$)	1.18 (**$2.80e^{-2}$**)	NA	NA
23	NA	$-5.97e^{-2}$ ($3.12e^{-1}$)	2.21 (**$1.00e^{-3}$**)	NA	NA

1277

9 | FIGURE CAPTIONS

FIGURE 1 Tooth identification within a jaw and landmarking. A) microCT image of a right lower jaw of a juvenile female *S. stellaris*, dorsal view. f, file as defined from the symphysis (dotted line) to the commissure; g, generation. Scale bar represents 5mm for the jaw and 3mm for the zoomed teeth; B) Examples of landmark (purple) and semilandmark (empty dots) setting on mesial (top) and distal (bottom) teeth of a juvenile female.

FIGURE 2 Palatoquadrate tooth shape diversity in *S. stellaris*. A-D) Hatchling female teeth; E-H) Juvenile female teeth; I-L) Mature female teeth; M-P) Mature male teeth. Symphyseal (mesial) pole to the left.

FIGURE 3 Meckelian tooth shape diversity in *S. stellaris*. A-D) Hatchling female teeth; E-H) Juvenile female teeth; I-L) Mature female teeth; M-P) Mature male teeth. Symphyseal (mesial) pole to the left.

FIGURE 4 Tooth dimensions of *S. stellaris* right Meckelian and palatoquadrate teeth. A and D) Morphometric measure of the ratio between main cusp height and crown base width; B and E) Deviation to tooth bilateral symmetry: difference between the tooth tip and each crown base extremity distances. C and F) Tooth centroid sizes. At each tooth position, mean values are computed among all tooth generations (internal replicates), before being computed among all specimens. Error bars are standard deviations among replicates and specimens.

FIGURE 5 2D representation (PC1xPC2) of tooth developmental trajectories in *S. stellaris*. A) 2D trajectories for palatoquadrate tooth files 3, 10, 15 and 20; B) 2D trajectories for Meckel's tooth files 1, 5, 15, and 20. The trajectory representations are drawn between the mean shape of hatchling (starting point), juvenile, and mature (arrow tip) specimen teeth. Purple and green shades are for females and males trajectories respectively. Mesial to distal files appear in light to deep shades. Wireframes depict extreme deformations of the mean shape at the positive and negative extremities of the PC1 and PC2 axes.

GRAPHICAL ABSTRACT

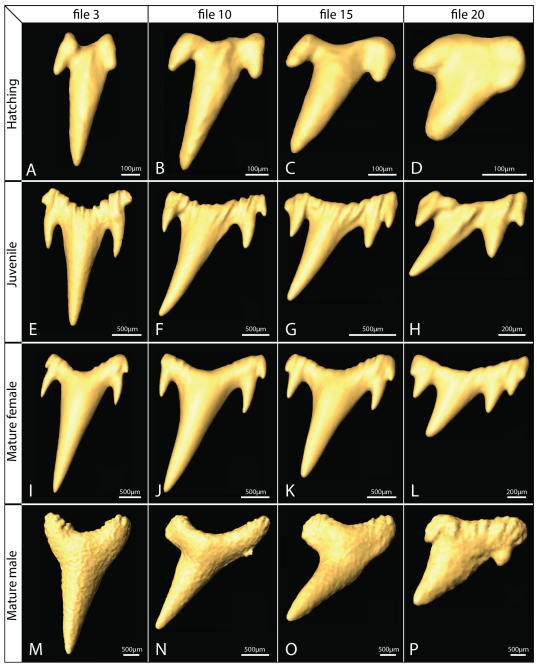

This study uncovers the wide intraspecific diversity of tooth form in the large-spotted catshark *Scyliorhinus stellaris* using micro-computed tomography and 3D geometric morphometrics. We characterize the emergence of sexual dimorphism along ontogenetic stages using sex-specific ontogenetic trajectories. We discuss the physical and chemical parameters acting on tooth morphogenesis that may generate the described developmental plasticity in elasmobranchs.